

Carbonatites from Eastern Paraguay and genetic relationships with potassic magmatism: C, O, Sr and Nd isotopes

F. Castorina¹, P. Censi², P. Comin-Chiaramonti³, E. M. Piccirillo⁴, A. Alcover Neto^{5,6}, C. B. Gomes⁷, T. I. Ribeiro de Almeida⁷, S. Speziale², and M. C. M. Toledo^{7,8}

¹ Dipartimento di Scienze della Terra, La Sapienza University, Roma, Italy

² Istituto di Mineralogia, Petrografia e Geo chimica, Palermo University, Italy

³ Dipartimento di Ingegneria Chimica, dell'Ambiente e delle Materie Prime, Trieste University, Italy

⁴ Dipartimento di Scienze della Terra, Trieste University, Italy

⁵ Centro de Tecnologia Mineral, CNPq, Ilha do Fundão, Rio de Janeiro, Brazil

⁶ Pós-Graduação, Instituto de Geociências, USP, São Paulo, Brazil

⁷ Instituto de Geociências, São Paulo University, USP, São Paulo, Brazil

⁸ NUPEGEL – Núcleo de pesquisas em Geoquímica e Geofísica da Litosfera, USP, São Paulo, Brazil

With 10 Figures

Received June 13, 1997;
accepted October 20, 1997

Summary

Geochemical characteristics were systematically determined for Early Cretaceous samples of carbonatitic rocks from Eastern Paraguay (Rio Apa, Amambay and Central Provinces). The data show that all the occurrences have an enriched isotopic signature and that the carbonatites have negligible or absent crustal signature. A petrogenetic model (parent liquids, fractional crystallization, hydrothermal interactions and weathering) is proposed as a function of incompatible trace element, stable (O-C) and radiogenic (Sr-Nd) isotope variations with the aim to test the significance of carbonatitic complexes as a marker of the metasomatized subcontinental lithospheric mantle. The results indicate that the carbonatites and primary carbonates from eastern Paraguay, and those from the north eastern Paraná Basin (SE Brazil), were affected by metasomatic events distinct in time and composition.

Zusammenfassung

Karbonatite aus Ost-Paraguay und ihre genetische Beziehung zu Kalium-Magmatismus: C, O, Sr und Nd Isotope

Die geochemischen Charakteristika von frühkretazischen Karbonatitproben aus Ostparaguay (Rio Alpa, Amambay und Zentrale Provinzen) wurden untersucht. Die Daten belegen, daß alle Vorkommen eine isotopische Anreicherungssignatur zeigen und daß ihnen eine entsprechende Krustensignatur fehlt. Ein Petrologisches Modell (Ausgangsschmelze, fraktionierte Kristallisation, hydrothermale Interaktion und Verwitterung) wird auf Grund der Verteilung der inkompatiblen Spurenelemente, der stabilen (C-O) und radiogenen (Sr-Nd) Isotope vorgeschlagen. Es versucht die Bedeutung der Karbonatitkomplexe als „Markerhorizonte“ des metasomatischen subkontinentalen Mantels zu überprüfen. Die Ergebnisse zeigen, daß die Karbonatite und die primären Karbonate in Ostparaguay, und jene aus dem Paraná Becken Südost-Brasiliens durch zeitlich und zusammensetzungsmäßig unterschiedliche metasomatische Prozesse erfaßt wurden.

Introduction

Carbonatitic rock-types from Southern Brazil (Paraná Basin) are associated with potassic complexes, of kama fugitic and plagioclacitic affinity, at the northern margins of the Paraná Basin (Fig. 1; Comin-Chiaromonti and Gomes, 1996; Morbidelli et al., 1995). These complexes, dated at 138 to 65 Ma (Rodrigues and Santos Lima, 1984; Comin-Chiaromonti and Gomes, 1996), appear to be related to the thermal perturbations responsible also for the flood tholeiites and alkaline magmatism of the Paraná Basin (Piccirillo and Melfi, 1988; Gibson et al., 1995; Morbidelli et al., 1995; Comin-Chiaromonti et al., 1997). The potassic magmatism and associated carbonatites from southern Brazil are believed to have originated from metasomatized mantle the melting of which would be triggered by the Tristan da Cunha (Huang et al., 1995) and Trindade (Gibson et al., 1995) mantle plumes, as also occurred for both the Paraná flood tholeiites and the associated alkaline rocks (Comin-Chiaromonti et al., 1997).

The genesis of carbonatites depends on processes such as liquid immiscibility, fractional crystallization and contamination by country rocks, whose role may be masked by hydrothermal and weathering processes. It is therefore essential to establish the primary geochemical features of carbonatites as these are crucial for evaluating their source(s).

The carbonatitic occurrences from Eastern Paraguay were investigated in terms of geochemistry, and O, C, Sr and Nd isotopes. Detailed petrography, mineral chemistry and major and trace element geochemistry are reported in Censi et al. (1989), Castorina et al. (1994, 1996), Comin-Chiaromonti et al. (1995) and Comin-Chiaromonti and Gomes (1996).

Geological setting

The carbonatite occurrences from Eastern Paraguay are associated with potassic complexes of plagioclacitic affinity (Comin-Chiaromonti et al., 1992, i.e. "Roman Province Type-Lavas", Comin-Chiaromonti and Gomes, 1996; Shaw,

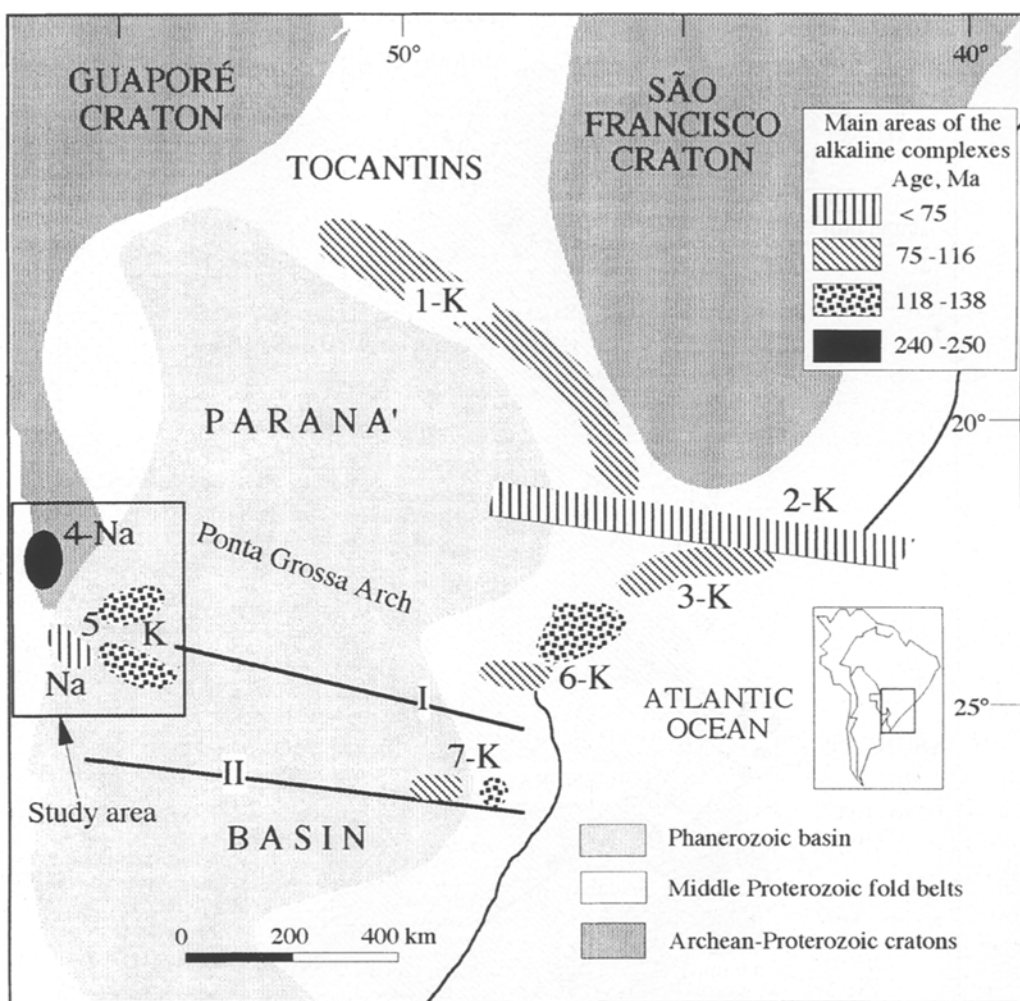
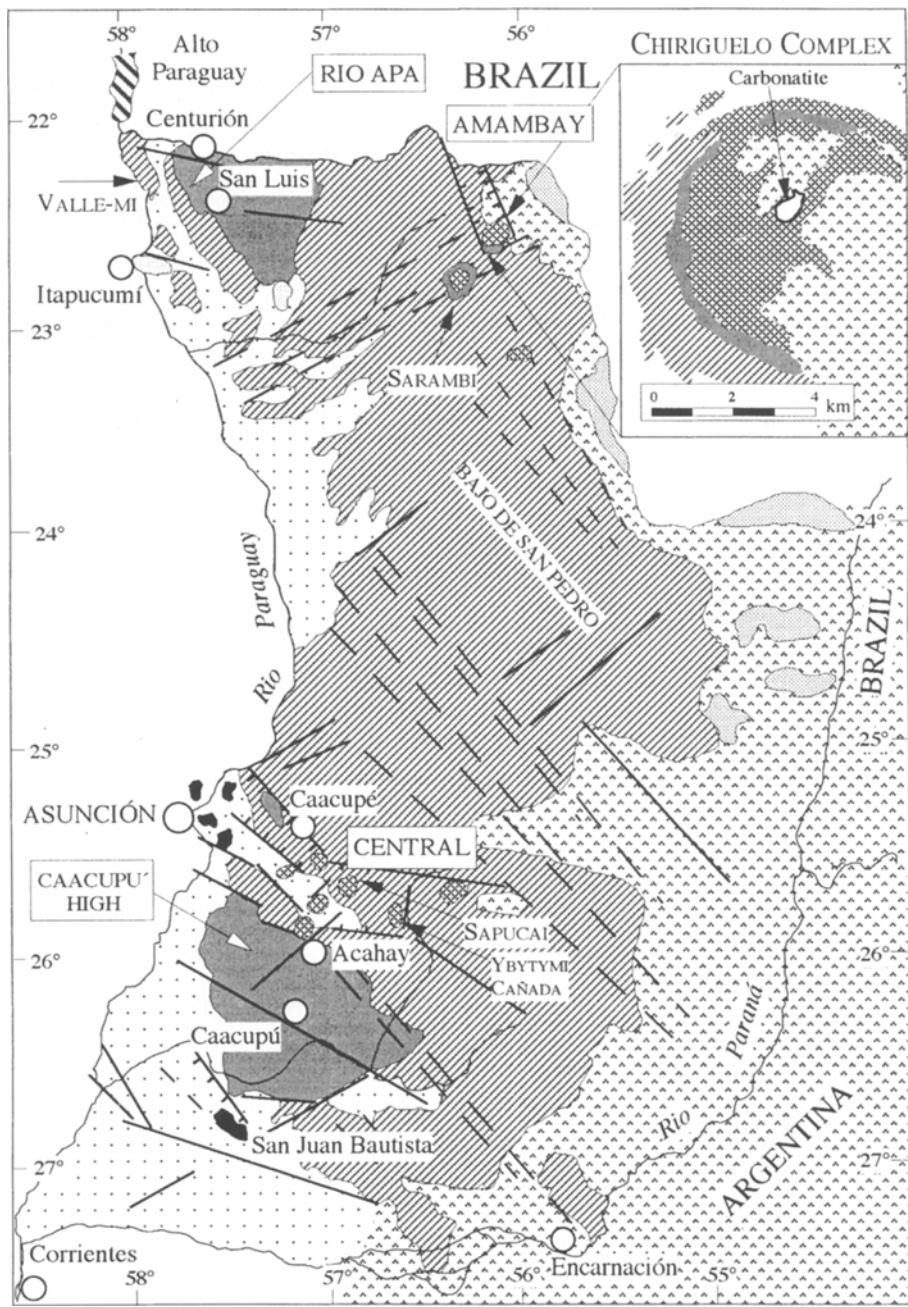


Fig. 1. Main areas of alkaline complexes in Brazil and Paraguay, in and around the Paraná Basin. *K* potassic, *Na* sodic rocks. 1 Alto Paranaíba (Morro do Engenho, Caiapó, Iporá, Santo Antonio da Barra, Catalao, Serra Negra, Salitre, São, Gotardo, Araxá, Tapira, poços de Caldas), 2 Taiuvá-Cabo Frio lineament (Taiuvá, Jaboticabal, Poços de Caldas, Passa Quatro, Itatiaia, Morro Redondo, Barra do Piraí, Tinguá, Canaa, Tanguá, Itaúna, Morro de São João, Cabo Frio), 3 Ribeira Belt (Ipanema, Piedade, Itanhaém, Ilha do Monte de Trigo, Ilha de São Sebastião, Ilha de Vitória, Ilha dos Búzios), 4 Alto Paraguay (Cerro Boggiani, Fecho dos Morros, Pão de Açucar, Cerro Siete Cabezas), 5 Paraguay (*K*: Apa, Chiriguelo, Sarambí, Acahay, Sapucai, Cañada, Ybytymí; *Na*: Ñemby, Lambaré, Tacumbú, Cerro Verde, Cerro Patiño, Villa Hayes), 6 Ponta Grossa Arch (Mato Preto, Barra do Itapirapuá, Itapirapuá, Tunas, Ponta Grossa, Jacupiranga, Juquiá, Cananéia), 7 Lages and Anitápolis. I, II: Rio Piquiri and Rio Uruguay lineaments, respectively (modified after Morbidelli et al., 1995). 1 and 7 kamafugitic affinity; 2, 3, 5 and 6 plagioclacititic affinity; 4 syenitic rock-types



- | | | | |
|---------------------|--|---------------------|---|
| [Dotted Pattern] | Tertiary-Quaternary alluvial cover | [Cross-hatching] | Early Cretaceous (137-133 Ma) flood tholeites ("Alto Paraná Formation" = Brazilian "Serra Geral Formation") |
| [Vertical Hatching] | Upper Cretaceous: aeolic sandstones ("Acaray Formation" corresponding to the bottom of the Brazilian "Bauru Group") | [Diagonal Hatching] | Late Permian-Early Triassic (250-240 Ma): mainly Na-syenites and effusive equivalents |
| [Solid Black] | Early Cretaceous (~120 Ma): nephelinitic plugs and dykes of San Juan Bautista. Palaeogene (70-32 Ma): nephelinitic and phonolitic lava flows, dykes and necks of Asunción area | [Diagonal Hatching] | Cambrian to Triassic-Jurassic: limestones, sandstones, arkoses, conglomerates, siltites, granitic intrusions and quartz-porphyry lava flows |
| [Cross-hatching] | Early Cretaceous (137-118 Ma) potassic rocks | [Wavy Line] | Precambrian-Cambrian crystalline basement: high-grade metasediments and granites |
| | | [Line with Dashes] | Graben |
| | | | Main faults |

Fig. 2. Generalized geological map of eastern Paraguay (*Comin-Chiaromonti et al., 1997*, modified). Inset: Sketch map of the Chiriguelo Complex (*Censi et al., 1989*, modified)

1996), in the westernmost side of the Paraná Basin. These complexes and the tholeiites of the Paraná Basin (Early Cretaceous) are more than 3200 and 5000 km from the supposed Trindade and Tristan da Cunha mantle plumes, respectively. The source mantle of the eastern Paraguay potassic rocks is constrained by high LILE, LREE, Th, U and K, which point to a lithospheric mantle source, i.e. "metasomatized" garnet peridotite (Comin-Chiaromonti et al., 1997).

In eastern Paraguay, the carbonatite occurrences crop out in three distinct provinces, i.e. Rio Apa, Amambay and Central Province (Fig. 2; Gomes et al., 1996). In the Rio Apa Province K-basanitic to phonotephritic dykes intrude limestones and dolostones of Early Ordovician age, near the Valle-mí township. The dykes contain irregular to round-globular large patches (ca. 15 wt%) of primary carbonates. In the Amambay Province the carbonatites are associated with the circular potassic complexes of Cerro Chiriguelo and Sarambí (Castorina et al., 1996). The Cerro Chiriguelo Complex (ca. 7.5 km across) is mainly formed by phonotephrites to high-K trachytes/phonolites surrounding a sōvitic core (cf. inset of Fig. 2). Notably, the circular structure is partially covered by the flood tholeiites of the Paraná Basin ($^{40}\text{Ar}/^{39}\text{Ar}$ dates: 133 ± 1 Ma; Renne, 1995, personal communication). Alvikitic stringers and late Fe-carbonatite veins crosscut the complex. The Sarambí Complex (ca. 7 km across), is characterized by high-K trachytic rocks intruded by pyroxenitic, sōvitic and silico-carbonatitic dykes and veins (Lechner-Wiens and Quade, 1990; Castorina et al., 1996). The Central Province represents the area with the major concentration of potassic complexes (Comin-Chiaromonti and Gomes, 1996). The carbonatite occurrences are scarce and virtually confined to the Sapucai Complex (Castorina et al., 1996), where silico-beforsitic flows and strongly carbonatated phonolitic dykes are present. Representative K/Ar dates (Table 1) are 137–138, 130–147 and 121–131 Ma for the Rio Apa, Amambay and Central Province, respectively. The preferred ages for the above three Provinces, are 137, 135 and 128 Ma, respectively.

Table 1. Representative K/Ar results for carbonatitic samples from eastern Paraguay. Data sources: (1) Velázquez and Capaldi, unpublished data; (2) Compte and Hasui, 1972; (3) Eby and Mariano, 1986; (4) Gomes et al., 1996

	Rock-type	Specimen	K wt%	$^{40}\text{Ar}_{\text{Rad}}$ 10^{-6}cSTPP/g	Ar atm%	Age
RIO APA						
VALLE-MÍ - STE-B (1)	Phonotephrite	Biotite	1.56	8.62	8.05	137 ± 7
VALLE-MÍ - STE-E (1)	Phonotephrite	Biotite	1.88	10.50	33.44	138 ± 9
AMAMBAY						
CHIRIGUELO (2)	Phonotephrite	Whole rock	7.11	39.90	13.70	139 ± 2
CHIRIGUELO (2)	Phonotephrite	Biotite	6.95	41.30	10.30	147 ± 9
CHIRIGUELO (3)	Silicocarbonatite	Whole rock				130 ± 5
ARROYO GASORY (3)	Trachyte	Biotite	7.71	43.25	12.25	135 ± 7
ARROYO GASORY (3)	Trachyte	Whole rock	6.15	34.85	25.22	136 ± 8
SARAMBÍ (1)	Glimmerite	Whole rock	7.08	40.14	28.44	136 ± 9
CENTRAL						
SAPUCAI (4)	Essexite	Whole rock	7.79	41.16	17.50	131 ± 8
SAPUCAI (4)	Phonolite	Whole rock	6.18	29.99	4.10	121 ± 4

Samples and methods

The samples studied are representative of the different carbonatitic and associated K-alkaline rocks from Eastern Paraguay. They include: (1) Rio Apa Province, alkaline dykes from Valle-mí; (2) Amambay Province, sôvites, alvikites and related silicate rocks from the Chiriguelo complex, both surface and borehole specimens; carbonatitic veins, pyroxenitic dykes and picritic xenoliths from the Sarambí complex; (3) Central Province, silico-beforsitic lava flows and phonolitic dykes from Sapucai complex and an ijolite from Cerro Cañada (cf. Fig. 2). Samples of limestones and dolostones of Early Ordovician age from the Valle-mí carbonate platform were also analyzed for comparison, as well as weathering and meteoric calcites from the Chiriguelo complex.

The procedure for Sr-Nd isotope measurements are given in *Castorina et al.* (1996). The $^{87}\text{Sr}/^{86}\text{Sr}$ and $^{143}\text{Nd}/^{144}\text{Nd}$ isotopic analyses were performed by means of a VG Isomass 54 E single collector and a Finnigan MAT 162 RPQ multi-collector mass spectrometer. Sr and Nd were separated from the matrix using ion exchange and reversed phase chromatography. REE were determined by inductively coupled mass spectrometry (ICP-MS; *Alaimo and Censi*, 1992). Carbonates for carbon and oxygen isotope analyses were reacted in duplicate with 100% H_3PO_4 at 25 °C for 1 day (calcite) and 3 days (dolomite), and with BrF_5 for 12 hours (oxygen for silicates) and analyzed by means of a Finnigan Mat Delta E mass spectrometer. The results are given in terms of the conventional $\delta\text{\textperthousand}$ units, reference standards being PDB-1 and V-SMOW for C and O isotopic compositions, respectively.

Analytical results

Sample location and the analytical results are listed in Table 2 (C-O isotopes) and Table 3 (Sr-Nd isotopes, Rb, Sr, La, Sm, Nd and ΣREE contents and La/Yb ratios). REE abundances are diagrammatically shown in Fig. 3.

Rare Earth Elements (REE)

The carbonatites and associated potassic rocks, mainly trachytes and trachy-phonolites/phonolites, have steep LREE-enriched patterns with respect to chondrites ($\text{La}_{\text{N}}/\text{Yb}_{\text{N}} = 18\text{--}282$). Lanthanum content ranges from 150 to 5000 times chondrites, and both the absolute REE contents and distribution patterns conform with those published for similar rock types (cf. *Andersen*, 1987; *Woolley and Kempe*, 1989). Notably, the carbonatites from the Chiriguelo and Sarambí complexes show a strong Eu negative spike, and a Sm-Eu positive spike, respectively, similar to those of the associated apatites (Fig. 3). The REE patterns suggest that apatite constrains the whole-carbonatite REE abundances, at least in the Chiriguelo and Sarambí complexes.

On the whole, the investigated samples cover the wide variation field of the carbonatites in terms of La vs La/Yb relationships (Fig. 4; *Andersen*, 1987). The carbonate fractions of alvikite and sôvite display higher La/Yb ratios (e.g. 266–330) and lower La (e.g. 250–390 ppm) contents than those of the corresponding

Table 2. Isotopic O-C values for carbonate and silicate phases from different rock-types from eastern Paraguay; (*), data in Livieres (1987). Cc Calcite; Dol dolomite; Cpx clinopyroxene (diopside wollastonite 0.5, enstatite 0.4); Ol, olivine (fo 86%); Bt, Biotite [Mg/(Mg+Fe²⁺)=0.7]. The standard deviation for the whole analytical procedure is about $\pm 0.05\text{‰}$ (1σ) for both carbon and oxygen isotopes

	$\delta^{18}\text{O}\text{‰}$ (V-SMOW)	$\delta^{13}\text{C}\text{‰}$ (PDB-1)		$\delta^{18}\text{O}\text{‰}$ (V-SMOW)	$\delta^{13}\text{C}\text{‰}$ (PDB-1)
RIO APA					
Valle-mí					
STE-A, Phonotephrite, Cc	17.12	-7.68			
STE-B, Phonotephrite, Cc	17.96	-6.82			
STE-C, Basanite, Cc	8.53	-7.30			
STE-D, Phonotephrite, Cc	18.30	-6.96			
STE-E, Phonotephrite, Cc	18.03	-7.75			
PS-279, Dolostone, Cc	23.88	-0.27			
Dol	20.55	-1.68			
PS-280, Limestone, Cc	22.85	0.57			
AMAMBAI					
<i>Chiriguelo Alkaline Complex</i>					
3407, Søvite, Cc	17.87	-7.01			
3408, Søvite, Cc	18.14	-5.97			
3409, Søvite, Cc	14.14	-6.30			
3410, Søvite, Cc	22.33	-4.71			
3411, Alvikite, Cc	15.93	-5.48			
3412, Søvite, Cc	17.76	-4.98			
3413, Søvite, Cc	16.21	-5.80			
3414, Alvikite, Cc	17.56	-5.75			
3416, Søvite, Cc	16.53	-6.40			
3417, Søvite, Cc	16.38	-4.98			
3418, Søvite, Cc	15.56	-6.74			
3419, Søvite, Cc	19.44	-3.97			
3420, Alvikite, Cc	15.45	-6.98			
3422, Alvikite, Cc	13.48	-7.26			
3423, D-trachyte, Cc	18.04	-6.89			
3433, Trachyte, Cc	18.71	-5.34			
3434, Søvite, Cc	11.22	-6.52			
3435A, Søvite, Cc	11.53	-7.77			
3435B, Søvite, Cc	14.94	-6.25			
3436, Søvite, Cc	12.51	-7.07			
3440, Fe-carbonatite, Cc	22.91	-4.10			
3442, Søvite, Cc	11.76	-8.08			
3443, Alvikite, Cc	13.07	-6.49			
K-1*	19.0	-5.1			
K-2*	12.8	-7.8			
K-3*	13.6	-7.1			
K-4*	17.4	-5.2			
K-5*	11.9	-7.3			
K-6*	21.9	-4.7			
K-7*	14.5	-6.7			
K-8*	14.0	-7.2			
<i>Chiriguelo, Well-24</i>					
49 (-93.5 m), Trachyte, Cc	12.36	-4.33			
50 (-97.5 m), Phonotephrite, Cc	13.55	-3.86			
51 (-101.2 m), Trachyphnolite, Cc	15.12	-0.62			
52 (-108.0 m), Trachyte, Cc	11.45	-4.86			
53 (-121.7 m), Trachyphnolite, Cc	11.04	-4.51			
54 (-136.8 m), Trachyte, Cc	11.04	-5.84			
55 (-142.0 m), Phonotephrite, Cc	13.25	-3.25			
56 (-155.2 m), Silicocarbonatite, Cc	10.99	-6.50			
57 (-175.0 m), Silicocarbonatite, Cc	14.96	0.14			
58 (-176.3 m), Phonotephrite, Cc	16.77	0.53			
59 (-183.6 m), Trachyte, Cc	18.47	1.12			
60 (-187.0 m), Silicocarbonatite, Cc	16.98	0.14			
61 (-197.0 m), Phonotephrite, Cc	18.53	1.12			
63 (-203.5 m), Trachyphnolite, Cc	15.06	-0.84			
64 (-233.0 m), Søvite, Cc	9.90	-7.40			
65 (-235.0 m), Trachyphnolite, Cc	12.87	-3.47			
68 (-294.0 m), Trachyphnolite, Cc	19.54	1.12			
69 (-333.0 m), Phonolite, Cc	11.79	-2.13			
70 (-361.0 m), Phonotephrite, Cc	13.55	-4.11			
71 (-387.0 m), Trachyte, Cc	12.67	-3.13			
AMAMBAI					
<i>Chiriguelo, Cc, late hydrothermal veins</i>					
CAU-08			23.62		-6.19
CHI-01			24.22		-3.98
CHI-02			23.21		-4.11
CHI-03			24.08		-4.55
CHI-05			22.40		-4.12
CHI-07			23.87		-6.45
CHI-12			22.77		-4.92
CHI-15			21.42		-3.71
CHI-16			24.04		-8.07
CHI-17			22.97		-4.47
CHI-19			23.77		-6.19
CHI-20			23.07		-6.24
CHI-21			22.29		-4.70
CHI-22			20.85		-2.31
CHI-23			21.79		-3.21
CHI-25			23.28		-5.26
CHI-27			23.40		-3.61
CHI-28			22.41		-9.10
<i>Weathering Calcites</i>					
CAU-9			16.21		-7.22
Chi-04			15.36		-5.38
Chi-06			16.79		-7.47
Chi-11			12.70		-6.06
Chi-18			17.80		-11.42
Chi-24			15.29		-8.86
Chi-26			13.29		-6.95
CAU-7f			17.10		-11.50
CAU-7g			16.69		-11.54
CAU-7h			18.39		-7.63
<i>Groundwater Calcites</i>					
Chi-13			27.21		-5.21
Chi-14			29.58		-8.13
CCh-20a			23.61		-4.58
CCh-20b			25.49		-5.55
CCh-20c			24.13		-4.37
CCh-20d			24.25		-4.31
CCh-05			28.09		-7.72
CCh-20e			24.80		-3.98
C-602			27.38		-4.70
C-700			24.98		-6.28
CCh-20f			25.20		-6.36
CCh-03			25.61		-6.24
<i>Sarambí Alkaline Complex</i>					
SA-90, Søvite, Cc			21.68		-5.68
SA-91, Silicocarbonatite, Cc			17.11		-10.37
SA-95, silicocarbonatite, Cc			14.96		-5.68
CENTRAL PROVINCE					
<i>Sapucaí Alkaline Complex</i>					
PS-72, Silicobeforsite, Dol			14.47		-5.63
PS-72, Silicobeforsite, Cc			14.00		-6.54
PS-94, Phonolite, Cc			16.70		-7.37
<i>Cañada Alkaline Complex</i>					
PS245, Ijolite, whole rock			5.91		
PS245, Cpx			5.20		
PS245, Bt			5.54		
PS245, Cc			6.90		-8.5
PS245, Ol			4.63		

Table 3. Selected trace elements (ppm) and isotope analyses of selected samples from eastern Paraguay. WR whole rock; Cc calcite; I. R. insoluble residuum (6.2 N HCl); Dol Dolomite. NBS-987 standard $^{87}\text{Sr}/^{86}\text{Sr}$ measured is 0.71027 ± 2 ($N=12$) and La Jolla standard $^{143}\text{Nd}/^{144}\text{Nd}$ measured is 0.51185 ± 1 ($N=5$). The reported uncertainties on Sr-Nd isotopic compositions represent in-run statistics at the 95% (2σ) confidence level. The ϵ' notations are from the following ages: Rio Apa, 137 Ma; Amambay, 135 Ma; Central, 128 Ma, and calculated using present day bulk-Earth parameters, i.e. UR = 0.7045 ($^{87}\text{Rb}/^{86}\text{Sr} = 0.0816$) and CHUR = 0.512638 ($^{147}\text{Sm}/^{144}\text{Nd} = 0.1967$). The isotope analyses were done at “Centro di Studio per il Quaternario e l’Evoluzione Ambientale”, CNR, Rome

	Rock-type	Rb	Sr	La	Sm	Nd	La/Yb	Σ REE	$^{87}\text{Sr}/^{86}\text{Sr}$	$^{143}\text{Nd}/^{144}\text{Nd}$	$\epsilon^{\text{t}}\text{Sr}$	$\epsilon^{\text{t}}\text{Nd}$	T ^{DM}
RIO APA													
STE-A Phonotephrite WR		20.8	2153	101	26.7	127.0	28.2	566	0.707683(7)	0.512059(8)	46.7	-10.1	1678
Cc (~15%)		4.9	1038	169	39.2	194.0	32.4	893	0.707698(41)	0.511937(5)	47.3	-12.4	1780
I.R.		23.6	2350	89	23.3	115.0	27.5	508	0.707643(7)	0.511961(8)	46.1	-11.9	1749
STE-B Phonotephrite WR	28.1	1926		21.7	114.0				0.707711(8)	0.511820(8)	46.7	-14.5	1828
Cc (~10%)		1.1	7092	130	27.3	147.9	30.9	646	0.707534(8)	0.511944(4)	45.3	-12.0	1602
I.R.		31.1	1352		23.3	110.0			0.707855(10)	0.511951(3)	48.1	-12.2	1867
STE-C Basanite WR	40.6	1151	149	23.8	148.7	57.1	667	0.707165(6)	0.511937(10)	37.3	-11.9	1424	
Cc (~15%)		0.9	12846	155	31.7	158.2	31.3	715	0.707059(10)	0.511935(12)	38.6	-12.4	1765
STE-D Phonotephrite WR	26.7	2212		22.6	104.8				0.708110(7)	0.511950(8)	52.5	-12.3	1915
Cc (~10%)		3.5	3354	143	35.8	155.9	26.7	732	0.707843(16)	0.511930(10)	49.6	-12.8	2142
I.R.		30.1	1974		21.1	98.2			0.708123(7)	0.511947(9)	52.5	-12.3	1910
STE-E Phonotephrite WR	31.1	2199		23.5	125.2				0.707111(10)	0.511951(8)	38.2	-11.9	1620
Cc (~20%)		26.8	1073	121	24.6	132.3	35.3	589	0.707100(15)	0.511930(10)	37.2	-12.3	1633
I.R.		32.2	2929		23.1	120.7			0.707165(6)	0.511971(7)	39.2	-11.6	1625
PS-279 Dolostone		4.9	272	1.05	0.15	0.60	35.0	3.8	0.70873(2)				
PS-280 Limestone		7.3	2670	0.86	0.46	0.48	14.3	3.7	0.70842(2)				
AMAMBAI													
Chiriguelo													
3409 Søvite WR	31.0	4158	1546	36.0	309.0	140.5	3521						
3411 Alvikite WR	24.0	2031	1257	33.0	181.0	96.7	2724						
3420 Alvikite WR	36.0	3129	1016	28.0	133.0	101.6	2134						
3422 Alvikite WR	39.0	5243	1169	30.0	178.0	146.1	3422						
Cc	17.8	5904	456	28.1	136.0	332.8	1213	0.707215(10)	0.511653(7)	40.5	-18.0	2267	
3423 D-Trachyte WR	218.0	500		77.0	405.0			0.70954(2)	0.511708(3)	39.4	-16.7	1983	
3424 D-Trachyte WR	256.0	543		64.1	358.0			0.70975(2)	0.511735(5)	39.6	-16.1	1832	
3434 Søvite WR	36.0	7441	590	20.0	120.0	98.3	1369						
Cc	31.4	11111	388	17.6	99.9	265.8	1132	0.707220(10)	0.511660(9)	40.6	-17.5	1902	
3435A Alvikite WR	39.0	9133	565	20.0	124.0	113.0	1325						
Cc	24.1	14520	250	14.4	79.9	305.0	769	0.707219(10)	0.511731(10)	40.7	-16.2	1849	
3435B Søvite WR	58.0	4397	1028	18.0	117.0	128.5	2075						
Cc	20.0	9972	304	24.2	88.0	330.4	916	0.70722(3)	0.511739(7)	40.7	-17.0	-	
3440 Fe-carbonatite WR	151.0	1776	312	12.0	110.0	78.0	655						
3442 Søvite Cc	27.1	17940	209	15.0	49.8	418.0	591	0.707218(10)	0.511659(9)	40.7	-18.8	-	
3443 Alvikite WR	59.1	7103	889	27.2	151.0	98.8	2170	0.707256(7)	0.511730(9)	40.7	-16.2	1849	
24-52 Trachyte WR	63.9	2187	66.4	10.8	66.5	57.7	275	0.707686(12)	0.511810(8)	45.2	-14.5	1594	
Cc	35.5	2923	152.9	14.8	74.5	118.5	497	0.707621(18)	0.511831(10)	45.6	-14.4	1900	
24-56 Si-carbonatite WR	341.0	8650	1651	162.6	1203	281.3	5322	0.707526(8)	0.511639(6)	42.1	-17.5	1593	
24-61 Phonotephrite WR	151.6	1731	112.8	10.9	118.2	42.71	592	0.708182(7)	0.511753(3)	47.6	-14.8	1254	
Cc	36.0	3158		10.1	56.38			0.707910(7)	0.511796(3)	49.7	-14.9	1751	
I.R.	667.4	1536		11.0	126.5			0.709859(18)	0.511782(13)	44.1	-14.2	1195	
24-64 Søvite WR	28.9	10300	1742	131.5	679.0	312.7	4578	0.707324(8)	0.511733(5)	42.1	-16.3	1987	
24-71 Trachyte WR	328.9	863	60.0	6.61	49.8	28.8	225	0.709628(10)	0.511799(7)	45.0	-14.4	1407	
Sarambí													
SA-95 Silicosøvite Cc	16.8	1065	159	26.1	42.1	62.4	420	0.70772(2)	0.511699(8)	46.7	-21.4	-	
GL-SA Glimmerite WR	138.1	1387		14.7	123.0			0.70817(2)	0.511463(3)	46.5	-20.8	1671	
Z1-A Pyroxenite WR	9.9	870			2.8	21.0		0.707245(10)	0.511471(9)	40.3	-20.8	1760	
CENTRAL													
Sapucai													
PS-72 Si-beforsite WR	148.0	1126	80	11.3	62.0			0.70807(2)	0.511804(6)	42.9	-14.8	1771	
Dol	3.2	106.4	239	19.1	159.9	75.6	928	0.70755(4)	0.511795(19)	43.2	-14.4	1336	
I.R.	227.0	1453		16.6	111.0			0.70820(3)	0.511800(15)	43.0	-14.6	1513	
PS-94 Phonolite Cc	6.3	103.7	76	2.3	18.7	126.7	203	0.70657(3)	0.512078(10)	27.0	-8.9	1066	
Cañada													
PS-245 Ijolite WR	114.0	1624	108	13.8	90.2	794	786	0.70737(2)	0.51192(1)	37.6	-12.3	1397	

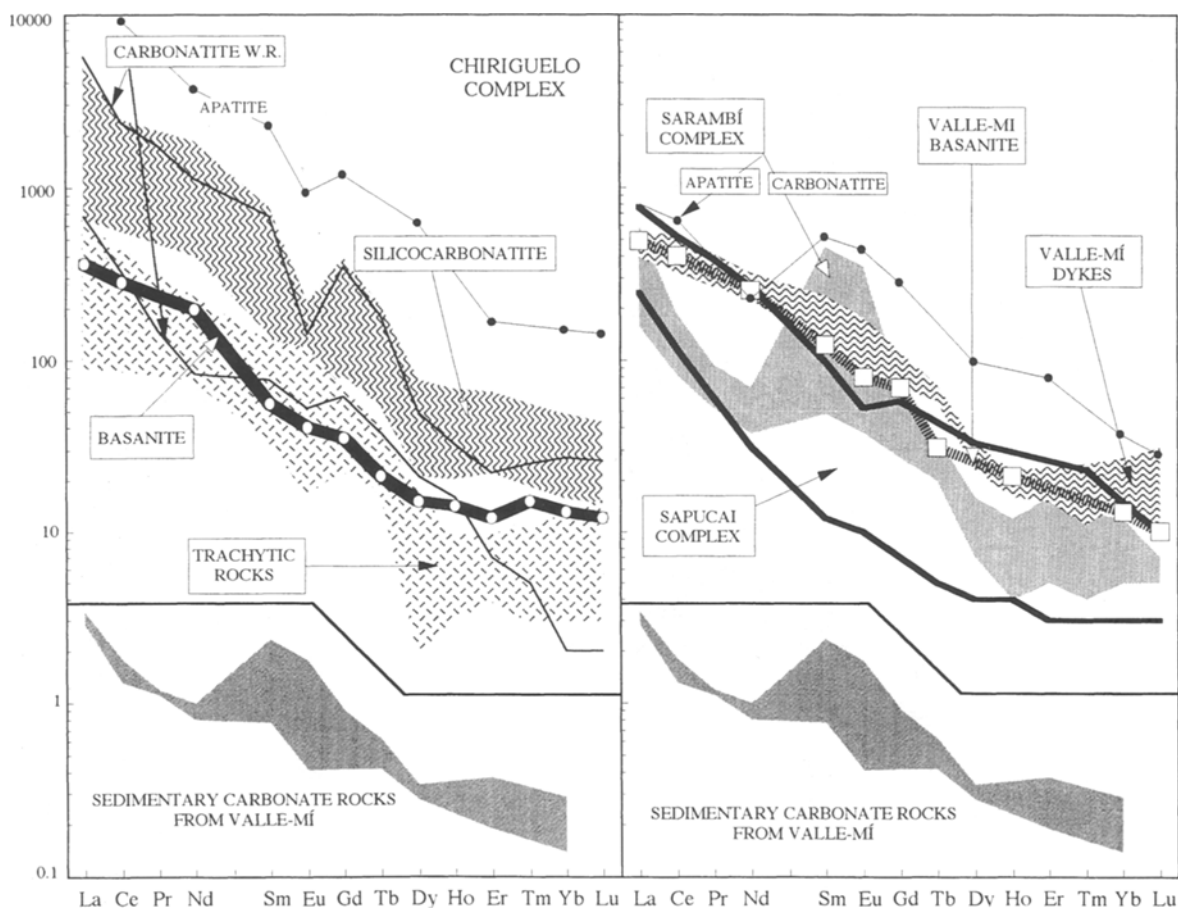


Fig. 3. Chondrite normalized (Boynton, 1984) REE distribution patterns for carbonatites and related rocks from Eastern Paraguay

host rocks ($\text{La/Yb} = 98\text{--}129$, $\text{La} = 565\text{--}1028 \text{ ppm}$). On the other hand, the carbonate fractions from the silicate rocks show both higher La and La/Yb than those of the corresponding silicate fractions (Table 3).

Figure 4 illustrates also the La vs La/Yb relationships for basanite-tephrite and phonolite-trachyte suites and associated primary carbonates. If the differentiation of the CO_2 -bearing parental magma is relatively restricted (i.e. basanite to phonotephrite), the exsolved carbonatitic melt is relatively small and crystallize forming groundmass patches. On the other hand, if the evolution from basic melts leads to phonolite or trachyte, the latter magmas may exsolve carbonatite melts characterized by high La and La/Yb relative to the parental fluid-rich basic magmas.

The mixing curves between parental magma(s) and the carbonatites (Fig. 4) provide an estimation of the CO_2 -rich melt fraction(s). Considering that the primary carbonates (up to 15–20 wt%) of the silicate rocks represent late crystallized phases, and that the carbonatites may represent the carbonatitic liquid exsolved from trachytic/phonolitic magma, the total carbonatitic magma appears to be higher than 30–35 wt% of the carbonate content in the parental silicate melt.

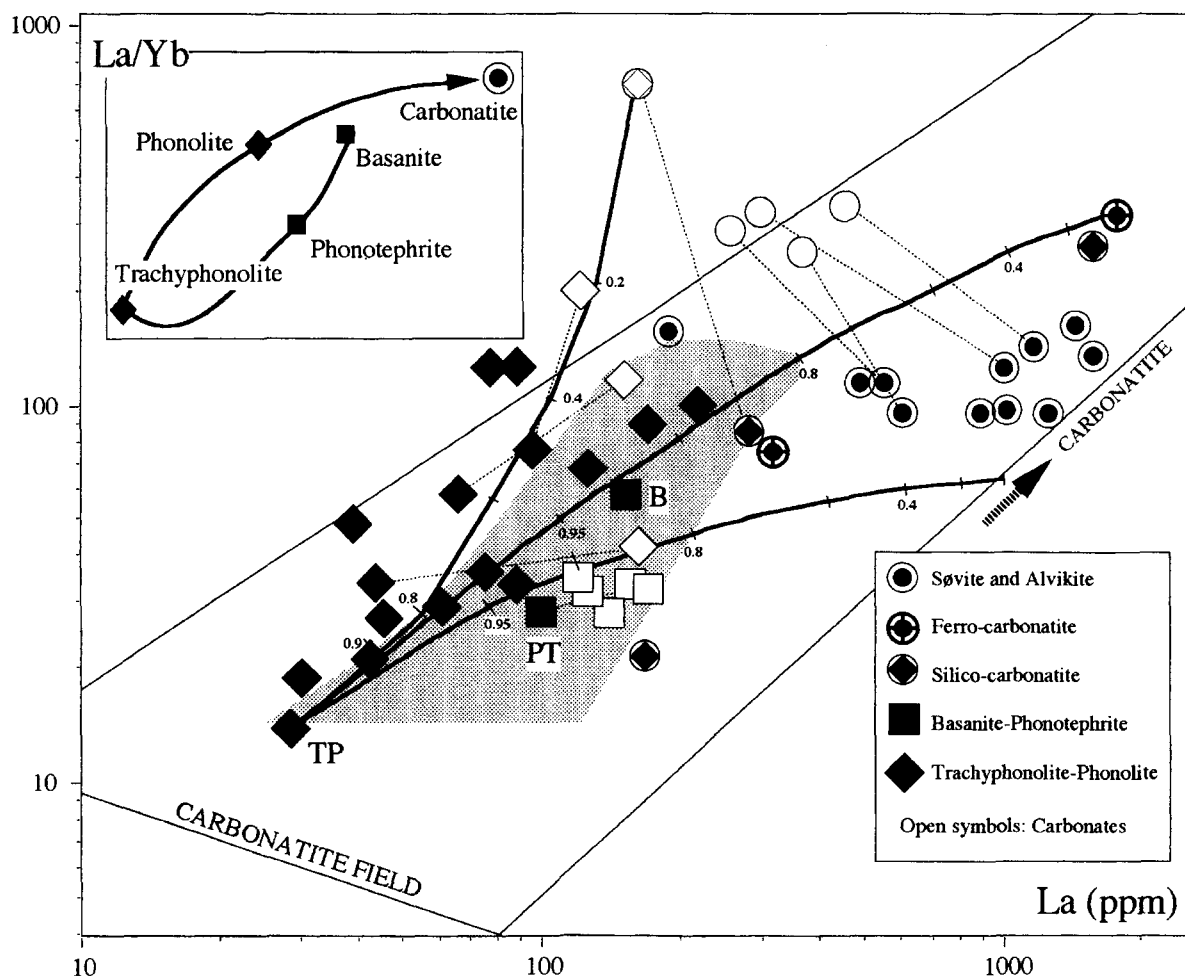


Fig. 4. La vs La/Yb ratios for the investigated samples (silicate rocks, carbonatites and carbonates) from eastern Paraguay; carbonatite field from Andersen (1987). Dotted area represents the limits of trachytic/phonolitic rock-types exsolving carbonatitic magma(s), as inferred by mixing (heavy) curves showing the fractions of residual liquid. Inset: evolution path from basanitic to carbonatitic magma

Thus, if for example, the basanite from Valle-mí (Rio Apa) is assumed as the parental magma of the carbonatites, the evolution consists of two main steps: (1) the first step (basanite \rightarrow trachyphonolite) leads to differentiated rock-types by crystal fractionation and allows the concentration of CO₂-rich fluids, and (2) the second one promotes the exsolution of about 20 wt% carbonatitic liquids from the differentiated phonolitic magma (cf. inset of Fig. 4).

It should be noted that both the parental magmas and most of the associated carbonatites plot within the “carbonatite field” of Andersen (1987). This suggests that the parental magmas of the carbonatites are characterized by high CaO/Al₂O₃, La/Yb and Ti/Eu (cf. Wallace and Green, 1988; Dautria et al., 1992; Dalton and Wood, 1993; Rudnik et al., 1993). CaO/Al₂O₃ vs La/Yb and Ti/Eu respectively (Fig. 5) show that the K-basanite-silico-carbonatite-carbonatite suites from Rio

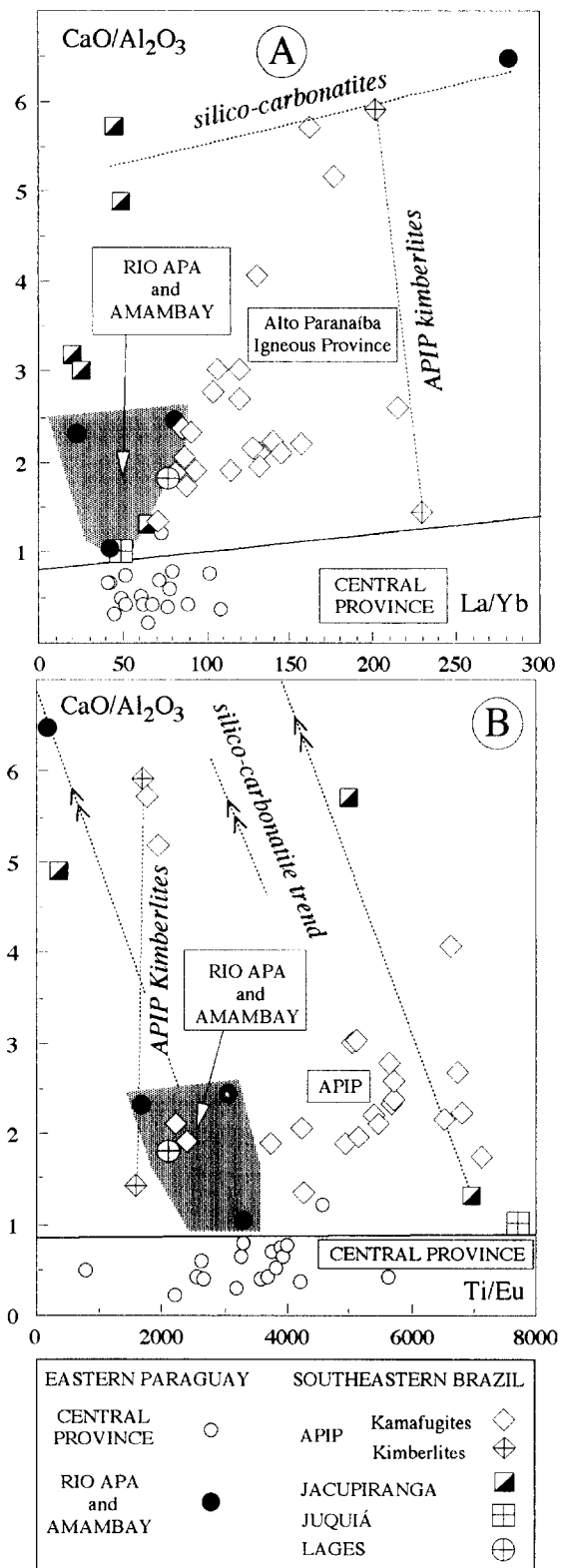


Fig. 5. Plot of $\text{CaO}/\text{Al}_2\text{O}_3$ vs La/Yb (A) and Ti/Eu (B) for the potassic rocks from eastern Paraguay and southeastern Brazil. APIP Alto Paranaíba Igneous Province (Gibson et al., 1995). Data sources: Castorina et al. (1994, 1996), Gibson et al. (1995), Comin-Chiaromonti and Gomes (1996), Traversa et al. (1996), Comin-Chiaromonti et al. (1997)

Apa and Amambay regions are characterized by $\text{CaO}/\text{Al}_2\text{O}_3$ increase, assisted by Ti/Eu decrease and La/Yb increase. It is notable that the K-basanites of the carbonatite suite have higher $\text{CaO}/\text{Al}_2\text{O}_3$ ratios relative to those of the Central Province and may, therefore, reflect mantle portions which underwent significant carbonatitic metasomatism. The initial stages of differentiation of the CO_2 -rich K-basanites are characterized by a silicate fraction which prevails on the carbonatitic component (cf. kamafugites from Alto Paranaíba, Brazil; Gibson et al., 1995) which, instead, are prominent on the last stages of differentiation.

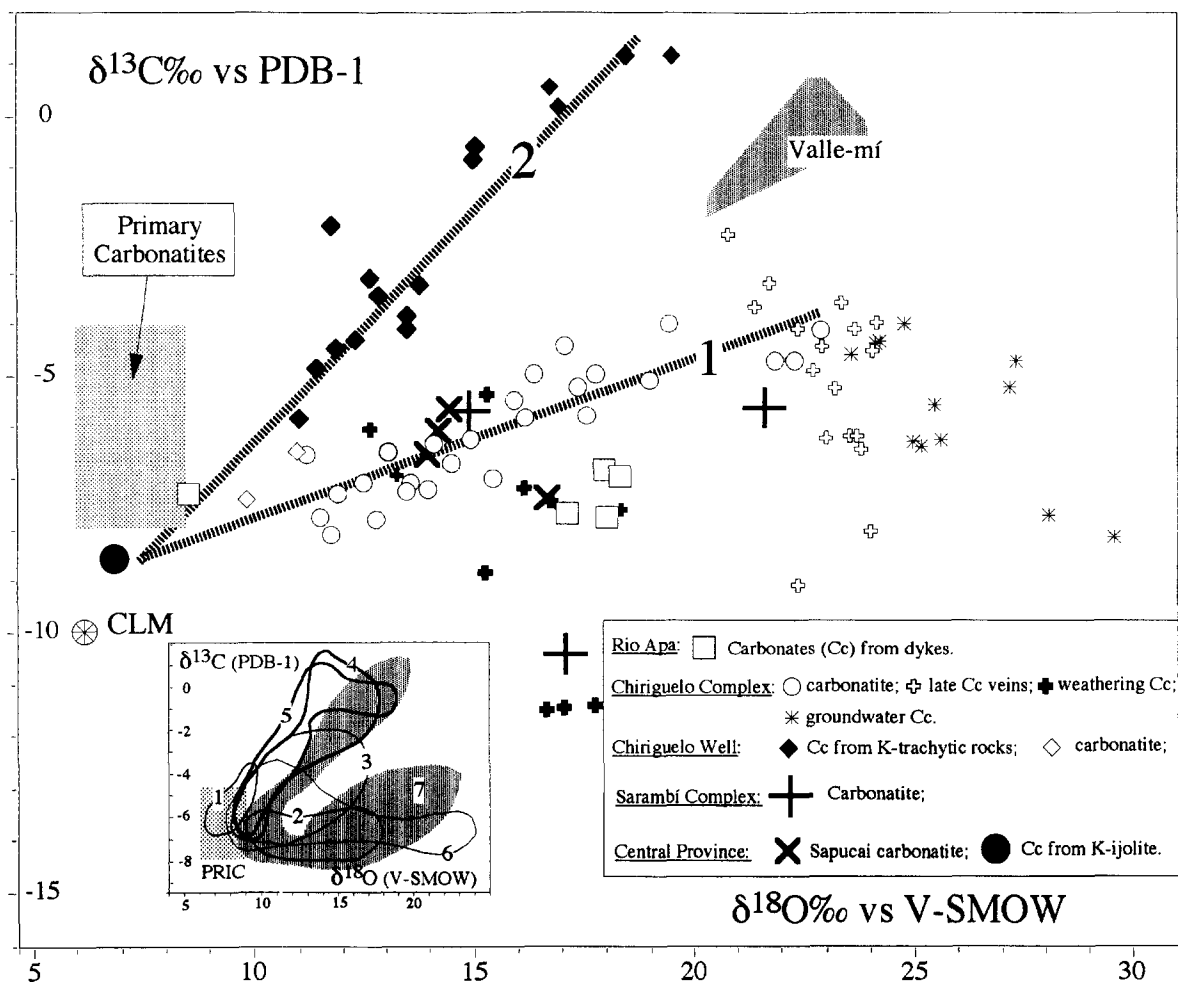


Fig. 6. Plot of $\delta^{13}\text{C}$ vs $\delta^{18}\text{O}$ for the carbonates and carbonatites from eastern Paraguay; dotted area: Valle-mí sedimentary carbonates; CLM continental lithospheric mantle (Kyser, 1990); Cc = Carbonates; 1 and 2 regression lines from field and borehole samples, respectively. Inset: comparison between the O-C isotopic compositions of carbonates from this study (dotted field: 7) and the isotopic compositions of carbonatites from southern Brazil; 1 Jacupiranga, 2 Juquiá, 3 Lages, 4 Barra do Itapirapuá, 5 Mato Preto, 6 Alto Paranaíba (Speziale et al., 1997; Censi and Comin-Chiaromonti, unpublished data). PRIC box of the "primary" carbonatites (Taylor et al., 1967)

Carbon and oxygen isotopes

The oxygen and carbon isotopic data are plotted in Fig. 6. $\delta^{18}\text{O}$ (V-SMOW) and $\delta^{13}\text{C}$ (PDB-1) values from magmatic carbonates mainly range between 6.5 and 24‰, and between –8 and 1‰, respectively. $\delta^{18}\text{O}$ and $\delta^{13}\text{C}$ from weathering calcites and meteoric calcites are in the ranges 13 to 18‰ and 23 to 30‰, and –11 to –5‰ and –8 to –4‰, respectively (Table 2). Note that the sedimentary carbonates from Valle-mí have $\delta^{18}\text{O}$ and $\delta^{13}\text{C}$ ranging from 20.6 to 23.9‰ and from –1.7 to 0.6‰, respectively, and that the isotopic C-O values of the carbonatites from eastern Paraguay overlap those from southern Brazil (inset of Fig. 6). The inset of Fig. 6 also shows two main areas of isotopic C-O variations for the Brazilian carbonatites. The first one (fields 1, 4 and 5; specimens from boreholes and/or mined quarries) is characterized by a shifting toward positive values of both $\delta^{18}\text{O}$ and $\delta^{13}\text{C}$. The second area (fields 2, 3, 6 and 7), which represents surface specimens, shows heavy O increase at similar values of $\delta^{13}\text{C}$.

Two main linear trends can be delineated for the carbonatitic rocks from eastern Paraguay. The first one is defined by the carbonates from silicate rocks of the Chiriguelo well (linear correlation coefficient: $r = 0.84$), while the second trend includes the magmatic carbonates of alvikites and sôvites (Censi et al., 1989) sampled near to, or at the topographic surface ($r = 0.86$). The two trends define an intercept at $\delta^{18}\text{O} = 7.45\text{\textperthousand}$ and $\delta^{13}\text{C} = -8.52\text{\textperthousand}$, corresponding to those of the primary carbonates ($\delta^{18}\text{O} = 6.9\text{\textperthousand}$ and $\delta^{13}\text{C} = -8.5\text{\textperthousand}$) of the K-ijolite from Cañada (eastern Paraguay, Central Province). These carbonates coexist with olivine ($\delta^{18}\text{O} = 4.63\text{\textperthousand}$), clinopyroxene ($\delta^{18}\text{O} = 5.20\text{\textperthousand}$) and biotite ($\delta^{18}\text{O} = 5.54\text{\textperthousand}$). In the Cañada K-ijolite, the silicate minerals show isotopic equilibration temperature of about 1200 °C (clinopyroxene-biotite = 1208 °C; clinopyroxene-olivine = 1201 °C; Bottinga and Javoy, 1975), whereas clinopyroxene-calcite pairs yielded an equilibration temperature of 690 °C (Matthews et al., 1983).

Strontium and neodymium isotopes

The Rb-Sr and Sm-Nd isotopic systematics of the investigated samples do not define isochrons (cf. Comin-Chiaromonti and Gomes, 1996), e.g. the Amambay samples ($n = 19$) yielded 131 ± 68 Ma. Assuming the ages in Table 3, the mean values for initial $^{87}\text{Sr}/^{86}\text{Sr}$ and $^{143}\text{Nd}/^{144}\text{Nd}$ ratios are, respectively: Rio Apa (137 Ma), $0.70749 (\pm 0.00039)$ and $0.51184 (\pm 0.00001)$; Amambay (135 Ma), $0.70738 (\pm 0.00022)$ and $0.51160 (\pm 0.00011)$; Central Province (128 Ma), (0.70713 ± 0.00032) and $0.51174 (\pm 0.00009)$. These Sr and Nd isotopic values do not result from crustal contamination, but reflect the “enriched component” of a metasomatized depleted mantle (Comin-Chiaromonti et al., 1995, 1997). Sr and Nd isotopes of carbonatites are consistent with those of the associated K-alkaline rocks (Fig. 7). Notably, alvikites of the Chiriguelo complex, which are believed to represent low-temperature hydrothermal conditions (Censi et al., 1989), are in the same Sr-Nd isotopic range of the main sôvite, whose carbonates recrystallized at high hydrothermal temperatures. Finally, the sedimentary carbonates from Valle-mí display $^{87}\text{Sr}/^{86}\text{Sr}$ (137 Ma) = 0.70850 (Table 3), while the Proterozoic crystalline basement has $^{87}\text{Sr}/^{86}\text{Sr}$ ratio of 0.71689 (Velázquez et al., 1996). In

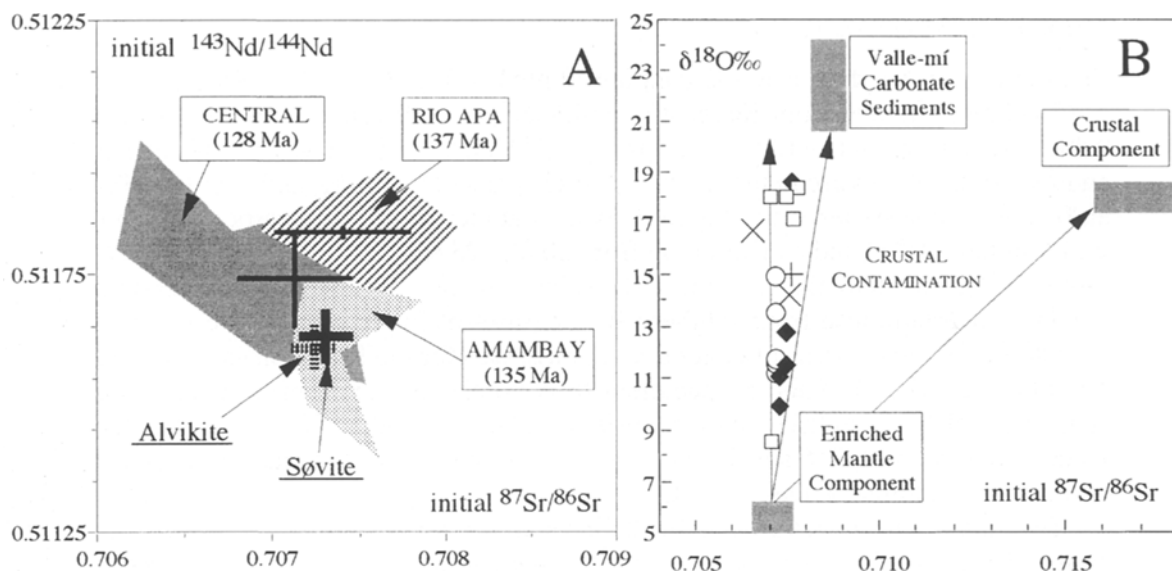


Fig. 7. A Initial $^{87}\text{Sr}/^{86}\text{Sr}$ vs $^{143}\text{Nd}/^{144}\text{Nd}$ ratios of potassic rocks from eastern Paraguay. Error bars represent the averaged values (with 1σ standard deviations) of the carbonates from the analyzed specimens. B Initial $^{87}\text{Sr}/^{86}\text{Sr}$ vs $\delta^{18}\text{O}\text{\%}$ for carbonatites from eastern Paraguay; symbols as in Fig. 6. Enriched mantle and crustal components are from Comin-Chiaromonti et al. (1997) and Velázquez et al. (1997), respectively; the range of the mantle component in terms of radiogenic Sr is the same (i.e. 0.70716 ± 0.00062) for all the potassic rocks from eastern Paraguay (Comin-Chiaromonti et al., 1995, 1997)

summary, Sr and Nd isotopes indicate that the investigated carbonatitic samples and associated potassic rocks were not affected by appreciable crustal contamination during their emplacement (Fig. 7B).

Discussion

In a previous paper based on surface specimens, Censi et al. (1989) showed that the C-O isotopic systematics of the carbonatitic rocks from the Chiriguelo complex reflected three main processes, i.e. (1) emplacement at shallow levels of søvites which reached $\delta^{18}\text{O}$ and $\delta^{13}\text{C}$ values of about 8.5\% and -6.5\% , respectively via distillation; (2) vapour exchange processes, which changed the latter $\delta^{18}\text{O}$ and $\delta^{13}\text{C}$ values to 20\% and -4.5\% , respectively, and (3) low ($\leq 50^\circ\text{C}$) temperature weathering, responsible for $\delta^{18}\text{O} = 23\text{\%}$ and $\delta^{13}\text{C} = -4.5\text{\%}$.

The samples from the Chiriguelo bore-holes and other carbonatitic occurrences from eastern Paraguay, allowed a further insight in the carbonatite magma genesis and evolution. Oxygen and carbon isotopes provided important informations about the evolution of a CO_2 -rich magma. This is discussed below, where the term “magmatic processes” is used to include partial melting, fractional crystallization and liquid immiscibility, “fluid processes” will refer to the interaction between rocks and fluids at different temperatures, including low-temperature weathering.

“Magmatic processes”

Assuming the K-ijolite PS-245 ($\text{mg\#} = \text{Mg}/(\text{Mg}+\text{Fe}^{2+}) = 0.68$; *Comin-Chiaromonti and Gomes, 1997*) as representative of an O-C near primary, mantle-derived melt (intercumulus calcite: $\delta^{18}\text{O} = 6.9\text{\textperthousand}$ and $\delta^{13}\text{C} = -8.5\text{\textperthousand}$, $\Delta\text{O} = 0.7$, $\Delta\text{C} = 1.5$, cf. *Kyser, 1990*), and that fractional crystallization + liquid immiscibility were responsible for variations not higher than 2\textperthousand both for $\delta^{18}\text{O}$ and $\delta^{13}\text{C}$ (cf. *Santos and Clayton, 1995*), the expected values for $\delta^{18}\text{O}$ and $\delta^{13}\text{C}$ should not exceed 9\textperthousand and $-6.5\text{\textperthousand}$, respectively.

The magmatic paths (see Appendix for calculation) may be related to two evolutionary steps, i.e. (a) partial melting of subcontinental mantle ($\delta^{18}\text{O} = 6.9\text{\textperthousand}$ and $\delta^{13}\text{C} = -10\text{\textperthousand}$) and differentiation of the primary magmas to the values of the K-ijolite PS-245 with $\text{CO}_2/\text{H}_2\text{O}$ ratio = 0.1, and (b) evolution with a $\text{CO}_2/\text{H}_2\text{O} \sim 0.2$ (shallow intrusion), and with a $\text{CO}_2/\text{H}_2\text{O} \sim 2.0$ (“surface” condition), respectively (Fig. 8).

“Fluid processes”

1. O-C modelling

After the crystallization of primary carbonates, the residual fluids may migrate and fenitize the country rocks, as well as the crystallized carbonates. The variations of O-C isotopes of neo-carbonates, due to the interaction between fluid and primary carbonates, will follow paths which depend on temperature and rock/water ratio (*Zheng and Hoefs, 1993*; cf. Appendix for details).

In Fig. 8 the variation paths relative to the O-C isotopic compositions during hydrothermal water-rock interaction are shown for a temperature range 400–100 °C (curve I, which fits the line 2 of Fig. 6), and 400–80 °C (curves II and III which enclose the straight line 1 of Fig. 6). Note that the low-temperature carbonates plot between curves II and III, or below III. The lowest values of $\delta^{13}\text{C}$ (enrichment in ^{12}C) may be related to hydrolysis of biogenic CO_2 . In this case, if the pH of the solutions is determined by humic acids, the ratio $[\text{HCO}_3^-]/[\text{Ca}^{++}]$ is a temperature function (cf. *Taylor, 1978* and *Usdowski, 1982*). For $\text{pH} \approx 5$ the major contribution of the biogenic component is at temperatures between 60 and 80 °C (Fig. 8).

2. Trace elements

In hydrothermal environments, the rock/water (R/W) interaction modifies the trace element content. Following *Nabelek (1987)*:

$$[\text{R}/\text{W}_{(\text{O})}]^{-1} = 1/\text{D} \left\{ \ln \left[\frac{\text{Cw}_i - \text{C}^{(\text{cc})}_i \text{D}}{\text{Cw}_i - \text{C}^{(\text{cc})}_f \text{D}} \right] \right\},$$

where Cw_i , $\text{C}^{(\text{cc})}_i$ and $\text{C}^{(\text{cc})}_f$ are the concentrations of a trace element in the fluid (w) and in the carbonate (cc), at the beginning (i) and at the end (f) of the interaction, respectively; $\text{D}[\text{C}_{wf}/\text{C}^{(\text{cc})}_f]$ is the ratio between a trace element in the fluid (wf) and in the carbonate (^{cc}f) at the end of the interaction. From calculated rock/fluid ratios (equation [8] in Appendix), and for fixed Cw_i , $\text{C}^{(\text{cc})}_i$ and $\text{C}^{(\text{cc})}_f$ values, the variation of a trace element and $\delta^{18}\text{O}$ is calculated by the above equation. According to *Nabelek's (1987)* model, the highest concentration of trace elements like Sr and REE are associated with temperatures higher than 200 °C.

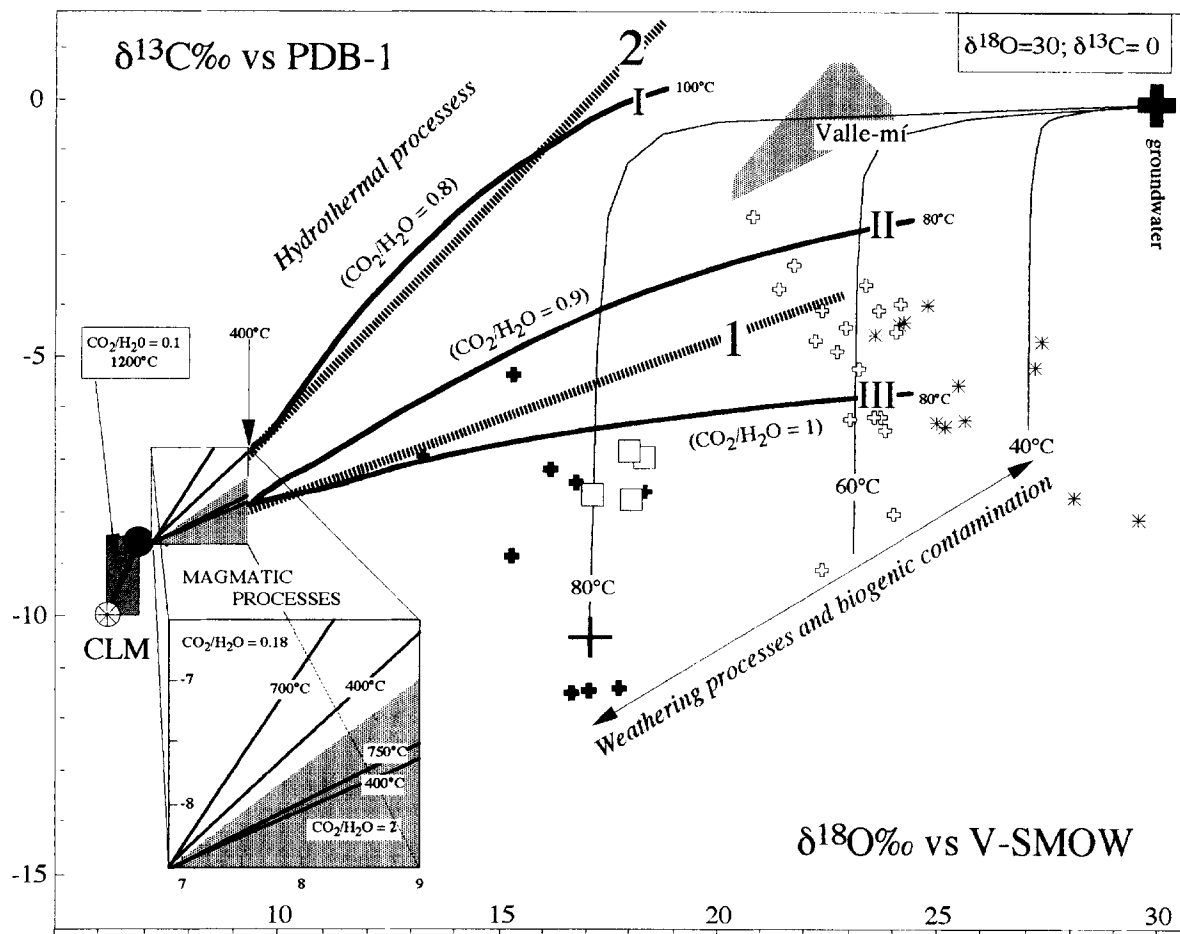


Fig. 8. Evolution of the C-O isotopic composition of calcite: magmatic conditions (i.e., 1200–400 °C), hydrothermal environment (I, up to 100 °C; II and III, up to 80 °C; see Appendix), and under low temperature conditions (biogenic component, pH ≈ 5, temperature = 40–80 °C; arbitrary starting composition, $\delta^{18}\text{O} = 30$, $\delta^{13}\text{C} = 0$, cf. Taylor, 1978 and Usdowski, 1982). CLM continental lithospheric mantle component. Symbols as in Fig. 6

The variation paths of $\delta^{18}\text{O}$ vs Sr, ΣREE contents (ppm) and La/Yb ratio are represented in Fig. 9. In the model $C_{\text{w}_i} > C_{\text{i}}^{(\text{cc})}$, i.e. “fenitizing” fluid enriched in incompatible elements with respect to the primary carbonates, according to the enrichment of halogens in the fluid and Sr, REE, and other elements as halogen-complexes (Wood, 1990; Bau, 1991; Rubin et al., 1993). In hydrothermal environments, the speciation of halogen-, hydroxide- and carbonate-complexes is a function of the pH range in the fluid (Haas et al., 1995). According to the interaction model of fluid-carbonatite, the pH range compatible with the system will depend on the $\text{CO}_2/\text{H}_2\text{O}$ ratio of the fluid, varying from 8.4–6.5 at 350 °C to 5.3–3.4 at 50 °C, respectively. It seems conceivable that a variable speciation in the hydrothermal fluid will start with REE strongly linked to hydroxides, and will stop with F-Cl-REE complexes at the end of the hydrothermal process (cf. Hass et al., 1995).

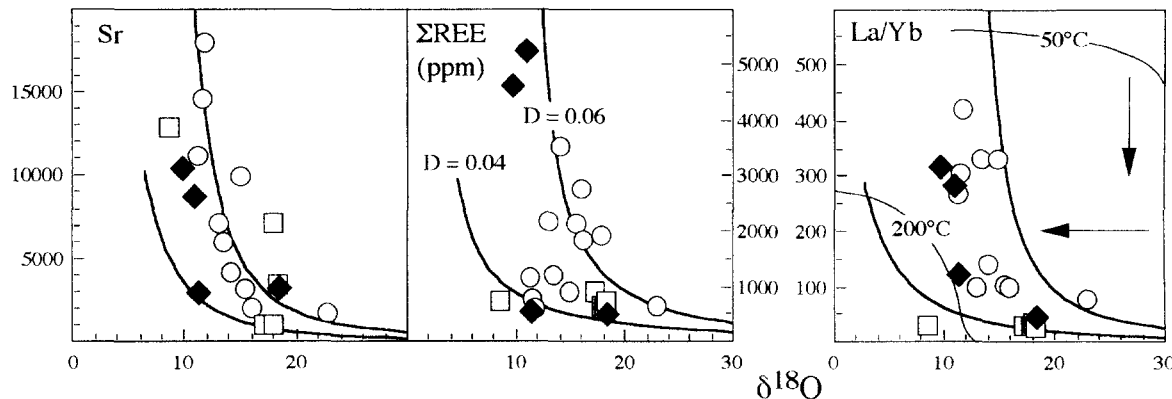


Fig. 9. Calculated paths of $\delta^{18}\text{O}$ vs Sr, ΣREE (ppm) and La/Yb ratio (heavy lines) in neo-carbonates, following fluid-rock interaction in a hydrothermal environment, compared with the analytical results; $D = \text{Cwf}/\text{C}^{(\text{cc})}\text{f}(\text{s.text})$. The temperature range is 200–50°C and the arrows show the trends of positive ΔT . Symbols as in Fig. 6

Mantle source characteristics

Typical specimens of potassic rocks from eastern Paraguay yielded initial $^{87}\text{Sr}/^{86}\text{Sr}$ (Sr_i) and $^{143}\text{Nd}/^{144}\text{Nd}$ (Nd_i) isotopic ratios within the ranges 0.70612–0.70754 and 0.51154–0.51184, respectively (Comin-Chiaromonti et al., 1997). These are similar to the associated carbonatites, but distinct (Fig. 10) from the potassic rocks and associated carbonatites from southern Brazil (Alto Paranaiba, Taiuvá-Cabo Frio, Ponta Grossa Arch and Lages). The latter rocks tend to plot toward the bulk Earth, while the eastern Paraguay analogues have higher Sr_i and lower Nd_i values and appear as an extension of the ‘‘Low Nd’’ array of Hart et al. (1986) in the enriched quadrant. Contamination models of the melts with crustal material imply unrealistic (up to 50%) contaminant fractions (Comin-Chiaromonti et al., 1997). Likewise, AFC processes do not account for the isotope data of the potassic rocks, given the poor correlations (not shown) between LILE and Sr_i and Nd_i . The data support the view that the potassic and carbonatitic rocks from eastern Paraguay, typically high in radiogenic Sr worldwide, represent the range of virtually uncontaminated magmas from this region.

Nd -model ages (inset B of Fig. 10) for potassic rocks from eastern Paraguay (depleted mantle: T^{DM}) range from 1.4 to 2.0 Ga (mean = 1.5 ± 0.2 Ga). In general, high-Ti and low-Ti uncontaminated tholeiites from the Paraná Basin (H-Ti and L-Ti, respectively; inset A of Fig. 10) show mean T^{DM} of 1.1 ± 0.1 and 1.5 ± 0.2 Ga, respectively. The range of model ages estimated for the potassic rocks implies that the corresponding melts derived from subcontinental mantle sources enriched by mantle ‘‘metasomatic processes’’ since Middle to Late Proterozoic times. These calculations require that Sm/Nd fractionation was not significant during magma genesis.

$T^{\text{DM}}(\text{Nd})$ model ages show that most potassic rocks and associated carbonatites from SE-Brazil range from 0.5 to 1.1 Ga. This range is virtually the same as that for high-Ti Paraná tholeiites. On the other hand, only the potassic rocks and

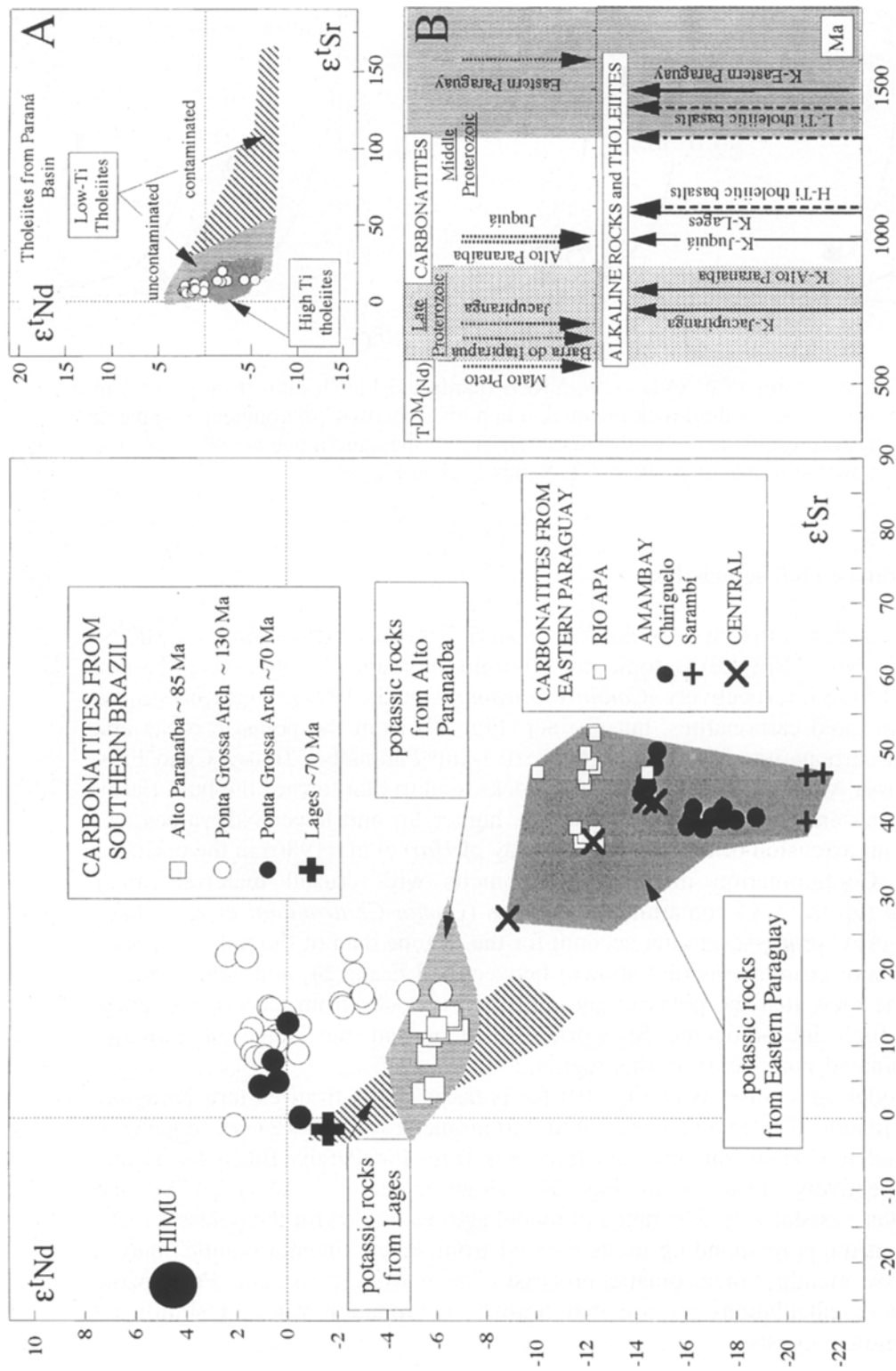


Fig. 10. Isotopic Sr-Nd correlations (ε^t notation) for igneous rocks from eastern Paraguay and southern Brazil. *Inset A*: Comparison between carbonatites and tholeiites of the Serra Geral Formation from Southern Brazil. Data sources: Piccirillo and Melfi (1988), Comin-Chiaromonti et al. (1991, 1992, 1995, 1997), Castorina et al. (1994, 1996), Gibson et al. (1995), Huang et al. (1995). *Inset B*: Mean model ages relative to carbonatites, potassic rocks and tholeiites in and around the Paraná Basin. The ε^t Sr and ε^t Nd were calculated using the following values for the Bulk Earth (Bell and Blenkinsop, 1989): $^{87}\text{Sr}/^{86}\text{Sr} = 0.7045$; $^{87}\text{Rb}/^{86}\text{Sr} = 0.0816$; $^{143}\text{Nd}/^{144}\text{Nd} = 0.512638$; $^{147}\text{Sm}/^{144}\text{Nd} = 0.1967$.

carbonatites from eastern Paraguay yielded T^{DM} of early Middle Proterozoic age, the same as most of the low-Ti uncontaminated Paraná tholeiites (*Comin-Chiaromonti et al.*, 1997).

These model ages indicate that two notional distinct mantle metasomatic events may have occurred during the Middle and Late Proterozoic as precursors to the potassic-carbonatitic and tholeiitic magmatism in the Paraná Basin. These metasomatic processes were chemically distinct, as indicated by the strong differences in Ti, LILE and HFSE concentrations between the alkaline rocks and tholeiites (low- vs high-Ti types) of the Paraná Basin (*Castorina et al.*, 1994, 1996; *Comin-Chiaromonti et al.*, 1997).

Conclusions

Significant variations in O-C isotope compositions occur in primary carbonates of potassic rock types from eastern Paraguay. These variations are mainly due to isotope exchange between carbonates and $\text{H}_2\text{O}-\text{CO}_2$ rich fluids, whereas magmatic processes, i.e. fractional crystallization or liquid immiscibility, probably affect the $\delta^{18}\text{O}$ and $\delta^{13}\text{C}$ values by not more than 2‰. The isotope exchange model implies that the main isotopic variations occurred at low temperature, in a hydrothermal environment, e.g. in the range 400–80 °C, involving fluids with a $\text{CO}_2/\text{H}_2\text{O}$ ratio ranging from 0.8 to 1. Two main paths of $\delta^{18}\text{O}-\delta^{13}\text{C}$ fractionation are generated by subvolcanic and surface conditions, respectively. Weathering and groundwater fluids, therefore, appear to be important, as well as meteoric water, which yielded samples strongly enriched in light carbon due to contamination by a biogenic component. The behaviour of trace elements (e.g. Sr and REE) is consistent with the above conclusions.

In general, Sr-Nd isotopes and trace-element data from potassic rocks from eastern Paraguay show that the associated carbonatites and associated primary carbonates reflect the composition of the source mantle. In particular, Sr and Nd isotopic data indicate that the carbonatite system is dominated by mantle component(s) without appreciable crustal contamination. Thus, in spite of the great variation shown by C-O isotopes due to “fluid processes”, Sr-Nd isotopic systematics can be related to an isotopically enriched source where the chemical heterogeneities reflect a depleted mantle “metasomatized” by small-volume melts and fluids rich in incompatible elements (*Castorina et al.*, 1994, 1996; *Comin-Chiaromonti et al.*, 1997). These are expected to have promoted crystallization of K-rich phases which gave rise to a veined network variously enriched in LILE and LREE. The newly formed veins (“enriched component”) and peridotite matrix (“depleted component”) underwent a different isotopic evolution with time which is reflected by the carbonatitic rocks. These conclusions may be extended to the whole Paraná Basin, where isotopically distinct alkaline and tholeiitic magmas were generated following two main “enrichment events” of the subcontinental lithospheric mantle at 2.0–1.4 and 1.0–0.5 Ga, respectively. The mantle sources preserved the isotopic heterogeneities over a long period of time, suggesting a non-convective (i.e. lithospheric) mantle beneath different cratons or intercratonic regions (*Comin-Chiaromonti et al.*, 1997).

Acknowledgements

We offer our thanks to *R. Alaimo* for the use of ICP-MS at CEPA Institution (Palermo, Italy). The “Universidad Nacionál de Asunción” is acknowledged for field assistance and the “Ministério de Obras Públicas y Comunicaciones del Paraguay” for drillhole samples. This research was supported by grants from Italian (CNR and MURST) and Brazilian (FAPESP) agencies.

Special thanks are due to *A. Cundari* and *A. R. Woolley* for their critical review and helpful suggestions. The constructive criticism of two *Mineralogy and Petrology* reviewers is also greatly appreciated.

References

- Alaimo R, Censi P* (1992) Quantitative determination of major, minor and trace elements on U.S.G.S. Rock standards by inductively coupled plasma mass spectrometry. *Atomic Spectrometry* 13: 113–11
- Andersen T* (1987) Mantle and crustal components in a carbonatite complex, and the evolution of carbonatite magma: REE and isotopic evidence from the Fen complex, southeast Norway. *Isotope Geosci* 65: 147–166
- Bau M* (1991) Rare earth elements mobility during hydrothermal and metamorphic fluid-rock interactions and the significate of the oxydation state of europium. *Chem Geol* 93: 219–230
- Bell L, Blenkinsop J* (1989) Neodymium and strontium isotope geochemistry of carbonatites. In: *Bell K* (ed) *Carbonatites: genesis and evolution*. Unwin Hyman, London, pp 278–300
- Bottinga Y* (1968) Calculation of fractionation factor from carbon and oxygen isotopic exchange in system calcite-carbon dioxide-water. *J Phys Chem* 72: 800–808
- Bottinga Y, Javoy M* (1975) Oxygen isotope partitioning among the minerals in igneous and metamorphic rocks. *Rev Geophys Space Phys* 13: 401–418
- Boynton WV* (1984) Cosmochemistry of the Rare Earth elements: meteorite studies. In: *Henderson P* (ed) *Rare Earth Element geochemistry*. Elsevier, Amsterdam, pp 63–114
- Castorina F, Censi P, Barbieri M, Comin-Chiaromonti P, Cundari A, Gomes CB* (1994) Carbonatites from the Paraná basin: a 130 Ma transect. In: International Symposium on the Physics and Chemistry of the Upper Mantle. São Paulo, Brazil. Extended Abstract, pp 52–55
- Castorina F, Censi P, Barbieri M, Comin-Chiaromonti P, Cundari A, Gomes CB, Pardini G* (1996) Carbonatites from Eastern Paraguay: a comparison with coeval carbonatites from Brazil and Angola. In: *Comin-Chiaromonti P, Gomes CB* (eds) *Alkaline magmatism in Central-Eastern Paraguay. Relationships with coeval magmatism in Brazil*. Edusp/Fapesp. São Paulo, Brazil, pp 231–248
- Censi P, Comin-Chiaromonti P, Demarchi G, Longinelli A, Orué D* (1989) Geochemistry and C-O isotopes of the Chiriguelo carbonatite, northeastern Paraguay. *J South Am Earth Sci* 3: 295–303
- Comin-Chiaromonti P, Gomes CB* (1996) Alkaline magmatism in Central-Eastern Paraguay. Relationships with coeval magmatism in Brazil. Edusp/Fapesp. São Paulo, Brazil, 464 pp
- Comin-Chiaromonti P, Civetta L, Petrini R, Piccirillo EM, Bellieni G, Censi P, Bitschene P, Demarchi G, DeMin A, Gomes CB, Castillo AMC, Velázquez JC* (1991) Tertiary nephelinitic magmatism in Eastern Paraguay: petrology, Sr-Nd isotopes and genetic relationships with associated spinel-peridotite xenoliths. *Eur J Mineral* 3: 507–525

- Comin-Chiaromonti P, Cundari A, Gomes CB, Piccirillo EM, Censi P, DeMin A, Bellieni G, Velazquez VF, Orué D* (1992) Potassic dyke swarm in the Sapucai graben, Eastern Paraguay: petrographical, mineralogical and geochemical outlines. *Lithos* 28: 283–301
- Comin-Chiaromonti P, Castorina F, Cundari A, Petrini R, Gomes CB* (1995) Dykes and sills from Eastern Paraguay: Sr and Nd isotope systematics. In: *Baer G, Heumann A* (eds) Physics and chemistry of dykes. Balkema, Rotterdam, pp 267–278
- Comin-Chiaromonti P, Cundari A, Piccirillo EM, Gomes CB, Castorina F, Censi P, DeMin A, Marzoli A, Speziale S, Velázquez VF* (1997) Potassic and sodic igneous rocks from Eastern Paraguay: their origin from the lithospheric mantle and genetic relationships with the associated Paraná flood tholeiites. *J Petrol* 38: 495–528
- Comte D, Hasui Y* (1971) Geochronology of Eastern Paraguay by the potassium-argon method. *Rev Bras Geoc* 1: 33–43
- Dalton JA, Wood BJ* (1993) The composition of primary carbonate melts and their evolution through wallrock reaction in the mantle. *EPSL* 119: 511–525
- Dautria JM, Dupuy C, Takherist D, Dostal J* (1992) Carbonate metasomatism in the lithospheric mantle: peridotitic xenoliths from a melilitic district of the Sahara Basin. *Contrib Mineral Petrol* 111: 37–52
- Eby NG, Mariano AN* (1986) Geology and geochronology of carbonatites peripheral to the Paraná Basin, Brazil-Paraguay. Carbonatites Symposium, Ottawa, pp 1–13
- Gibson SA, Thompson RN, Leonardos OH, Dickin AP, Mitchell JG* (1995) The Late Cretaceous impact of the Trindade mantle plume; evidence from large-volume, mafic, potassic magmatism in SE Brazil. *J Petrol* 36: 189–229
- Gomes CB, Comin-Chiaromonti P, Velázquez VF, Orué D* (1996) Alkaline magmatism in Paraguay: a review. In: *Comin-Chiaromonti P, Gomes CB* (eds) Alkaline magmatism in Central-Eastern Paraguay. Relationships with coeval magmatism in Brazil. Edusp/Fapesp, São Paulo, Brazil, pp 31–58
- Haas JR, Shock EL, Sassani DC* (1995) Rare earth elements in hydrothermal systems: estimates of standard partial molar thermodynamic properties of aqueous complexes of rare earth elements at high pressures and temperatures. *Geochim Cosmochim Acta* 59: 4329–4350
- Harned HS, Davis R* (1943) The ionization constant of carbonic acid in water and the solubility of carbon dioxide in water and aqueous salt solution from 0° to 50 °C. *J Am Chem Soc* 65: 2030
- Hart RS, Gelarch DC, White WM* (1986) A possible Sr-Nb-Pb mantle array and consequences for mantle maxing. *Geochim Cosmochim Acta* 50: 1551–1557
- Huang H-M, Hawkesworth CJ, Van Calsteren P, McDermott F* (1995) Geochemical characteristics and origin of the Jacupiranga Carbonatites, Brazil. *Chem Geol* 119: 79–99
- Jacobson RL, Langmuir D* (1974) Dissocation constants of calcite and CaHCO_3^+ from 0° to 50 °C. *Geochim Cosmochim Acta* 38: 301–312
- Kyser TK* (1990) Stable isotopes in the continental lithospheric mantle. In: *Menzies MA* (ed) Continental mantle. Clarendon Press, Oxford, pp 127–156
- Lechner-Wiens H, Quade H* (1990) Geologische-Petrographische Darstellung des Alkali-intrusivkomplexes "Cerro Sarambi" in Ost Paraguay. Geowissenschaftliches Latinamerika Kolloquium, München (Abstract)
- Livieres-Guggiari RA* (1987) Der Karbonatit – Komplex von Chiriguelo, Nordost-Paraguay. Thesis, Clausthal Technical University, Germany, 191 pp
- Matthews A, Goldsmith JR, Clayton RN* (1983) Oxygen isotope fractionations involving pyroxenes: the calibration of mineral-pair geothermometers. *Geochim Cosmochim Acta* 47: 631–644

- Mattey DP, Taylor WR, Green DH, Pillinger CT* (1990) Carbon isotopic fractionation between CO₂ vapour, silicate and carbonate melts: an experimental study to 30 kbar. *Contrib Mineral Petrol* 104: 492–505
- Mook WG, Bommerson JC, Staverman WH* (1974) Carbon isotope fractionation between dissolved bicarbonate and gaseous carbon dioxide. *EPSL* 22: 169–176
- Morbidelli L, Gomes CB, Beccaluva L, Brotzu P, Conte AM, Ruberti E, Traversa G* (1995) Mineralogical, petrological and geochemical aspects of alkaline and alkaline-carbonatite associations from Brazil. *Earth Sci Rev* 30: 135–168
- Nebelek PI* (1987) General equation for modeling fluid/rock interaction using trace elements and isotopes. *Geochim Cosmochim Acta* 51: 1765–1769
- O'Neil JR* (1986) Theoretical and experimental aspects of isotopic fractionation. In: *Valley JW, Taylor HP, O'Neil JR* (eds) Stable isotopes in high temperature geological processes. *Rev Mineral* 16: 1–40
- O'Neil JR, Clayton RN, Mayeda TK* (1969) Oxygen isotope fractionation in divalent metal carbonates. *J Chem Phys* 51: 5547–5558
- Piccirillo EM, Melfi AJ* (1988) The Mesozoic flood volcanism from the Paraná basin (Brazil). Petrogenetic and geophysical aspects. Iag-Usp, São Paulo, Brazil, 600 pp
- Rodrigues CL, Dos Santos Lima PRA* (1984) Carbonatitic complexes of Brazil. Companhia Brasileira de Metalurgia e Mineração São Paulo, Brazil, pp 3–17
- Rubin JN, Christopher DH, Price JG* (1993) The mobility of zirconium and other “immobile” elements during hydrothermal alteration. *Chem Geol* 110: 29–47
- Rudnik RL, McDonough WF, Chappell BW* (1993) Carbonatite metasomatism in the northern Tanzanian mantle: petrographic and geochemical characteristics. *EPSL* 114: 463–475
- Shaw CSJ* (1996) The petrology and petrogenesis of Roman Province-Type Lavas and ultrapotassic leucitites. In: *Mitchell RH* (ed) Undersaturated alkaline rocks: mineralogy, petrogenesis, and economic potential. Mineral Ass Canada, Winnipeg, Manitoba, pp 175–192
- Speziale S, Censi P, Ruberti E, Gomes CB, Comin-Chiaromonti P* (1997) Isotopic O-C fractionation in carbonatites: evidences from Barra do Itapirapuá and Mato Preto Complexes (Southern Brazil). *Mineral Petrogr Acta* (submitted)
- Santos RV, Clayton RN* (1995) Variations of oxygen and carbon isotopes in carbonatites: a study of Brazilian alkaline complexes. *Geochim Cosmochim Acta* 59: 1339–1352.
- Taylor HOJr* (1978) Water/rock interactions and origin of H₂O in granitic batholiths. *J Geol Soc London* 133: 509–558
- Taylor HPJr, Frechen J, Degens ET* (1967) Oxygen and carbon isotope studies of carbonatites from Laacher See district, West Germany and Alnø district, Sweden. *Geochim Cosmochim Acta* 31: 407–430
- Traversa G, Barbieri M, Beccaluva L, Coltorti M, Conte AM, Garbarino C, Gomes CB, Macciotta G, Morbidelli L, Ronca S, Scheibe LF* (1996) Mantle sources and differentiation of alkaline magmatic suite of Lages, Santa Catarina, Brazil. *Eur J Mineral* 8: 193–208
- Usdowski E* (1982) Reaction and equilibria in the system CO₂-H₂O and CaCO₃-CO₂-H₂O(0°–50°). A review. *N Jb Mineral Abh* 144: 148–171
- Velázquez VF, Gomes CB, Teixeira W, Comin-Chiaromonti P* (1996) Contribution to the geochronology of the Permo-Triassic alkaline magmatism of the Alto Paraguay Province. *Rev Bras Geoc* 26: 103–108
- Wallace ME, Green DH* (1988) Mantle metasomatism by ephemeral carbonatite melts. *Nature* 336: 459–462

- Woolley AR, Kampe DRC (1989) Carbonatites: nomenclature, average chemical compositions, and element distribution. In: Bell K (ed) Carbonatites, genesis and evolution. Unwin Hyman, London, pp 1–14
- Wood SA (1990) The aqueous geochemistry of the rare earth elements and yttrium, 2. Theoretical prediction of speciation in hydrothermal solutions to 350 °C at saturated water pressure. Chem Geol 88: 99–125
- Zheng YF, Hoefs J (1993) Carbon and oxygen isotopic convariations in hydrothermal calcites. Theoretical modeling on mixing processes and application to Pb-Zn deposits in the Harz Mountains, Germany. Mineral Deposita 28: 79–89

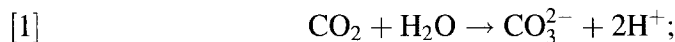
Appendix

Isotopic O-C modelling for magmatic and hydrothermal evolution of carbonatitic rocks was carried out using Microsoft Excel 5 programs (*Speziale et al.*, 1997). The programs are available on request as worksheet from Dr. P. Censi (Istituto di Mineralogia, Petrografia e Geo chimica, Università di Palermo, via Archirafi, 36, I-90123, Palermo, Italy).

“Magmatic processes”

The following hypotheses are considered for the modellization of Fig. 8:

- (A) partial melting of a garnet-peridotite (cf. *Comin-Chiaromonti* and *Gomes*, 1996);
- (B) evolution of the liquid by fractional crystallization at a temperature of about 1200 °C in a closed system, CLM to PS-245 (Canada K-ijolite, Central Province, Eastern Paraguay) composition and a final temperature between 750–400 °C;
- (C) primary carbonate crystallization from a hypercritical CO₂-H₂O-rich liquid, according to the relationship:



- (D) CO₂ and H₂O are the only O-C sources in the system;
- (E) mass balance:

$$[2] \quad 2\mathbf{A}\delta^{18}\text{O}_{(\text{CO}_2)}^i + \mathbf{C}\delta^{18}\text{O}_{(\text{H}_2\text{O})}^i = 2\mathbf{a}\delta^{18}\text{O}_{(\text{CO}_2)} + 3\mathbf{b}\delta^{18}\text{O}_{(\text{cc})} + \mathbf{c}\delta^{18}\text{O}_{(\text{H}_2\text{O})}$$

and

$$[3] \quad \mathbf{A}\delta^{13}\text{C}_{(\text{CO}_2)}^i = \mathbf{a}\delta^{13}\text{C}_{(\text{CO}_2)} + \mathbf{b}\delta^{13}\text{C}_{(\text{cc})}$$

where **a**, **b**, **c** are CO₂, CO₃²⁻ and H₂O molar concentrations in the system at time t ≠ “i” (initial time), **A**, **C** are the initial CO₂ and H₂O concentrations at “i” before the crystallization of the carbonate, cc represents the isotopic composition of the carbonate {i. e., fixed **A**, from CO₂/H₂O initial ratio, **C** is defined}; in this case [2]–[3] have a behaviour in which the values of the various components will be defined for each “t” from **b**=**A-a** and **c**=**C-b**}, and it follows that the isotopic composition of the carbonate can be determined by the isotopic fractionation factors Δ¹⁸O_(CO₂-cc), Δ¹⁸O_(cc-H₂O), Δ¹³C_(CO₂-cc) (*Bottinga*, 1968;

O'Neil et al., 1986):

$$[4] \quad \delta^{18}\text{O}_{(\text{cc})} = [2\mathbf{A}\delta^{18}\text{O}_{(\text{CO}_2)}^{\text{i}} + \mathbf{C}\delta^{18}\text{O}_{(\text{H}_2\text{O})}^{\text{i}} - 2\mathbf{a}\Delta^{18}\text{O}_{(\text{CO}_2-\text{cc})} \\ + \mathbf{c}\Delta^{18}\text{O}_{(\text{cc}-\text{H}_2\text{O})}] / [3\mathbf{b} + 2\mathbf{a} + \mathbf{c}]$$

$$[5] \quad \delta^{13}\text{C}_{(\text{cc})} = [\mathbf{A}\delta^{13}\text{C}_{(\text{CO}_2)}^{\text{i}} - (\mathbf{A} - \mathbf{b})\Delta^{13}\text{C}_{(\text{CO}_2-\text{cc})}] / \mathbf{A}$$

"Fluid processes"

The equations, according to *Zheng and Hoefs (1993)*, are:

$$[6] \quad \delta^{18}\text{O}_{(\text{cc})} = (\delta^{18}\text{O}_{(\text{H}_2\text{O})}^{\text{i}} + \Delta^{18}\text{O}_{(\text{cc}-\text{H}_2\text{O})}) \\ - [(\delta^{18}\text{O}_{(\text{H}_2\text{O})}^{\text{i}} + \Delta^{18}\text{O}_{(\text{cc}-\text{H}_2\text{O})}) - \delta^{18}\text{O}_{(\text{cc})}^{\text{i}}] \exp(-R/W_{(\text{O})})$$

$$[7] \quad \delta^{13}\text{C}_{(\text{cc})} = (\delta^{13}\text{C}_{(\text{HCO}_3)}^{\text{i}} + \Delta^{13}\text{C}_{(\text{cc}-\text{HCO}_3)}) - [(\delta^{13}\text{C}_{(\text{HCO}_3)}^{\text{i}} \\ + \Delta^{13}\text{C}_{(\text{cc}-\text{HCO}_3)} - \delta^{13}\text{C}_{(\text{cc})}^{\text{i}}) \exp(-R/W_{(\text{C})}\chi_{(\text{HCO}_3)})]$$

where $\delta^{18}\text{O}_{(\text{cc})}, \delta^{13}\text{C}_{(\text{cc})}$: calcite O-C starting isotopic values; $\delta^{13}\text{C}_{\text{HCO}_3}^{\text{i}}$: initial C-value of HCO_3^- in the fluid; $\chi(\text{HCO}_3)$: HCO_3^- molar fraction in the fluid; $R/W_{(\text{O})}$ and $R/W_{(\text{C})}$ rock/water ratios for O and C, respectively, defined as (Kps being the calcite solubility product):

$$[8] \quad R/W_{(\text{O})} = 3\text{Kps}/\{[\text{H}_2\text{O}][\text{CO}_3^{2-}]\};$$

$$[9] \quad R/W_{(\text{C})} = \text{Kps}/\{[\text{H}_2\text{CO}_3] + [\text{HCO}_3^-]\}[\text{CO}_3^{2-}], R/W = f(T^\circ\text{K}),$$

according to *Jacobson and Langmuir (1974)*:

$$[10] \quad \log \text{Kps} = -13.870 - 3059/T^\circ\text{K} - 0.04035^*T^\circ\text{K}$$

Also HCO_3^- , molar fraction in the fluid, is $f(T^\circ\text{K})$, because the constants of the equilibria: $\text{CO}_2 + \text{H}_2\text{O} \leftrightarrow \text{H}_2\text{CO}_3(K_0)$ and $\text{H}_2\text{CO}_3 \leftrightarrow \text{H}^+ + \text{HCO}_3^-(K_1)$ are $f(T^\circ\text{K})$, and, following (*Harned and Davis, 1943*):

$$[11] \quad \log K_0 = -14.0184 + 2385.73/T^\circ\text{K} + 0.0152642^*T^\circ\text{K},$$

$$[12] \quad \log K_1 = -14.8435 + 3404.71/T^\circ\text{K} - 0.032786^*T^\circ\text{K},$$

C speciation depending on temperature. The $\delta^{13}\text{C}_{(\text{HCO}_3)}^{\text{i}}$, initial isotopic composition, is then calculated from isotopic fractionation according to *Mook et al. (1974)*, for various $\delta^{13}\text{C}$ of CO_2 in the fluid.

Authors' addresses: *F. Castorina*, Dipartimento di Scienze della Terra, Università "La Sapienza", Piazzale Aldo Moro 5, I-00185 Rome, Italy; *P. Censi* and *S. Speziale*, Istituto di Mineralogia, Petrografia e Geochimica dell'Università, Via Archirafi 36, I-90100 Palermo, Italy; *P. Comin-Chiaromonti*, Dipartimento di Ingegneria Chimica, dell'Ambiente e delle Materie Prime dell'Università, Piazzale Europa 1, I-34127 Trieste, Italy; *E. M. Piccirillo*, Dipartimento di Scienze della Terra dell'Università, Via E. Weiss 8, I-34127 Trieste, Italy; *A. Alcover Neto*, *C. B. Gomes*, *T. I. Ribeiro de Almeida* and *M. C. M. Toledo*, Instituto de Ciências, Universidade de São Paulo, Caixa Postal 11348, 05422-970 São Paulo, SP, Brazil.